1-1-1989

Variable Structure and Ultimate Boundedness control and stabilization of flexible robotic systems

Perumal Jegan Nathan
University of Nevada, Las Vegas

Order Number 1338268

Variable Structure and Ultimate Boundedness control and stabilization of flexible robotic systems

Nathan, Perumal Jegan, M.S.

University of Nevada, Las Vegas, 1989

U·M·I
300 N. Zeeb Rd.
Ann Arbor, MI 48106

VARIABLE STRUCTURE AND ULTIMATE BOUNDEDNESS CONTROL AND STABILIZATION OF FLEXIBLE ROBOTIC SYSTEMS

by
Perumal J. Nathan

A thesis submitted in partial fulfillment
of the requirements for the degree of

Master of Science

in

Electrical Engineering

Department of Computer Science and Electrical Engineering
University of Nevada Las Vegas
August, 1989

The thesis of Perumal Jegan Nathan for the degree of Master of Science in Electrical Engineering is approved

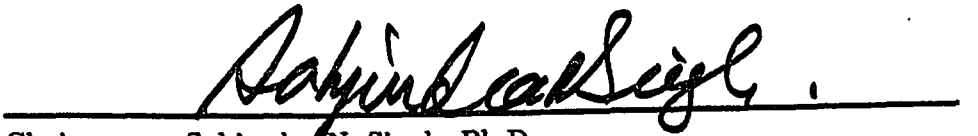

Chairperson, Sahjendra N. Singh, Ph.D.

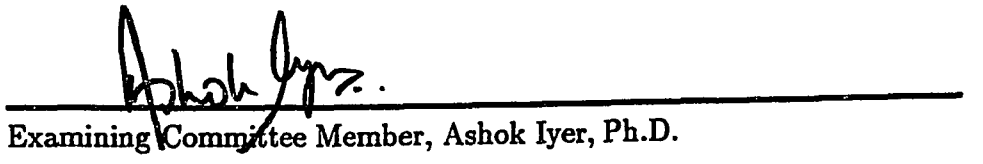

Examining Committee Member, Ashok Iyer, Ph.D.

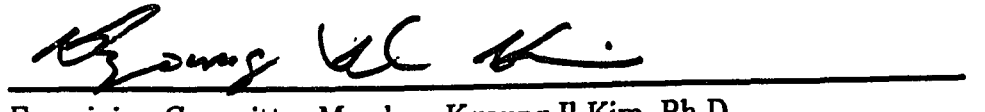

Examining Committee Member, Kyoung Il Kim, Ph.D.

Graduate Faculty Representative, William G. Culbreth, Ph.D.

Graduate Dean, Ronald W. Smith, Ph.D.

University of Nevada Las Vegas
August, 1989

Acknowledgement

It is my great pleasure to thank Professor Sahjendra N. Singh for his untiring guidance in making me understand the principles involved in this thesis work besides the course work which he taught to get the grasp of the nonlinear control theory during my enrollment at UNLV. My special thanks are due to Dr. Ashok Iyer for his support and guidance throughout my graduate study. I would like to thank Dr. Kyoung I. Kim for his guidance in understanding the principles of digital signal processing and applications and I thank Dr.William G. Culbreth for his willingness to be my thesis committee member. I also would like to thank Mr. R. Srinivasan and Dr. N. Saikia of Hindustan Aeronautics Ltd., my ex-bosses who continued to give me moral support and encouragement in my effort to do the graduate studies. With great pleasure I would like to thank my wife, Premalatha for her understanding, patience and prayers throughout my studies at Las Vegas.

Finally, I wish to thank the Army Research Office for providing financial support for my graduate study at UNLV, without which I would not have achieved this milestone in my academic endeavor.

Abstract

In this thesis we study the control of two link light weight elastic manipulator in the presence of uncertainty. The control of flexible robotic arm with uncertainty such as variable payload, joint angle frictional torque etc., is an interesting and important problem. The equation of motion of robotic systems are highly nonlinear and coupled. The design of controllers for rigid manipulators behave poorly in the presence of structural flexibility. Hence it becomes necessary to design control systems which include the interaction of the rigid and elastic modes.

Here we consider control of joint angles and stabilization of the flexible modes caused by the manuever of robotic arm by two methods. These are : (i) Variable Structure control and (ii) Nonlinear Ultimate Boundedness control. The Variable Structure control which is a discontinuous control, is evolved in two phases, namely the "reaching phase" and the "sliding phase". Nonlinear Ultimate Boundedness control is a continuous control wherein the joint angle tracking error is uniformly ultimately bounded in the closed-loop system.

Analytical derivations of these two schemes are presented in this thesis for the control of two-link flexible arm and feedback stabilizers are designed for each scheme based on the linear models using pole assignment technique to dampen the elastic oscillations of the links. A control logic is included which switches the stabilizer when the joint angle trajectory enters

a specified neighborhood of the terminal state.

Extensive simulations were carried out for several conditions of uncertainty and the results are presented. The results of implementation of variable structure joint angle control of a single-link arm using a digital signal processor is also presented at the end.

Contents

List of Figures

Chapter 1

Introduction

The design of light weight robotic arm is of current interest, and is attracting the attention of many researchers. Such manipulators are energy efficient and achieve high performance compared to manipulators with rigid links. Light weight robot structures are also desirable for space applications. However, lighter member of robot arms are more likely to elastically deform while manuever which yields dynamic deflection. This elastic vibration persists for a period of time after a move is completed. The settling time required for this residual vibration delays subsequent operations, thus conflicting with the demand for increased productivity. Furthermore the static deflection due to varying payload causes inaccuracies in positioning. These conflicting requirements between high speed and high accuracy have rendered a challenging research problem. For high speed maneuver, mechanism should be made light weight to reduce the driving torque requirements and to enable the robot arm to respond faster. Hence it is necessary to obtain an accurate dynamic model of a flexible

structure, with all the coupling terms between the flexible and rigid body motions need to be retained. In this thesis a detailed model of two link flexible robot was developed on the basis of the work done by Maizza-Neto [1] before the development of control schemes.

The controllers of industrial manipulators are designed on the assumption that the links are rigid. However, controllers designed for rigid robotic systems perform poorly in the presence of structural flexibility, and it becomes necessary to design control systems which include the interaction of the rigid and elastic modes. Such a design is complicated due to the presence of uncertainty (such as variable payload, joint frictional torques,etc) in the system. The equations of motion of robotic systems are highly nonlinear and coupled, and this further complicates the design problem. Hence a sophisticated controller design is needed to ensure the desired performance of the robot.

For the last few years, research effort has been made to design control systems for robotic systems which have flexible links. Based on linearized models, several control systems have been designed. Ref. [1-8] lists the work carried out in the control of flexible robot on the basis of linearized model. In these work it was assumed that all the states are available for the closed loop control system. This includes the flexible motion in the control action, thus achieving positional accuracy with the existing joint torquer. However in practical situation, not all states would be available for closed loop feed back control. Since the above system does not take in to account the nonlinearities of the dynamic model the design of controller is an approximation and hence the performance is not accurate. Based on nonlinear inversion and stabilization, nonlinear control systems for elastic robotic systems have been

presented in [13-15]. This work takes in to account the stabilization of flexible motion and static deflections with the feedback of elastic states. This concept gives the control system designer more capabilities to improve the robot arm with additional force actuators at the tip of the flexible link.

A singular perturbation strategy has been used to design controllers based on the seperation of slow and fast modes [16-18]. In singular perturbation strategy the fast state variables are the elastic forces and their time derivatives. In this way two reduced order systems are identified ; a slow subsystem that of rigid manipulator and a fast subsystem that of elastic forces. Hence a slow control is designed for rigid manipulator and a fast control is designed for the elastic motion.

A nonlinear controller for large uncertainty has been designed in [19]. Experimental results related to control of flexible arm have also been reported in literature [9-12]. All of these experiments were carried out for a single flexible link manipulators in the horizontal plane to avoid gravitational effect.

In this thesis, we present nonlinear control systems based on the variable structure system (VSS) and ultimate boundedness control (UBC) which accomplish asymptotic decoupled joint angle trajectory tracking. Once the trajectory reaches the neighborhood of terminal joint angles, a stabilizer using pole placement which is designed on the linearized model about the terminal state is closed to control the elastic oscillations of the links. Extensive simulations were carried out with varying payload and joint mass inertia and the results show that the controllers exhibit robustness toward payload uncertainties.

Chapter 2

Mathematical Model and Problem formulation

2.1 The Physical Model

The schematic of the general physical system is shown in Figure 1. The system is composed of two flexible links connected by a frictionless pinned joint. One end of the first link is attached to the origin of a reference frame and the other end is attached to the second link. The links are assumed to have planar motion and the relative motion of the two links result from torques applied at each joint of the link. In this figure, OXY is an inertial frame with origin at joint 1, OX_1Y_1 is a reference frame with axis X_1 tangent to link 1 at O, and $O_2X_2Y_2$ is a reference frame with origin at joint 2 with its axis X_2 tangent to link 2 at point O_2. The axis OX points vertically down. Figure shows arm lying along OO_2O_p in a deformed position. However, if they were rigid, the arm would lie along OO_1O_3. Let θ_1, θ_2 be the joint angles of this hypothetical rigid arm.

2.2 Equation of Motion

In order to write the equation of motion of the proposed system, we make use of the so called assume-mode method (cantilever). Based on this method the elastic deflection of the arm is denoted as $\delta_1(l_1,t)$ for link 1 at a distance l_1 from O_1 along OX_1 and $\delta_2(l_2,t)$ for link 2 at distance l_2 from O_2. These elastic deflections can be represented as

$$\delta_1(l_1,t) = \sum_{i=1}^{n} \phi_{1i}(l_1) p_{1i}(t) \tag{2.1}$$

$$\delta_2(l_2,t) = \sum_{i=1}^{n} \phi_{2i}(l_2) p_{2i}(t)$$

where ϕ_{1i} and ϕ_{2i}., $i = 1,...,n$, are appropriately chosen basis functions; p_{kj}, $k = 1,2$; $j = 1,...,n$, are the generalized coordinates; and n denotes the number of elastic modes retained in this representation.

In this study, it is assumed that longitudinal and torsional deformations are negligible. The mode shapes ϕ_{ij} (admissible functions) are assumed to be the eigenfunctions of a clamped-free beam. This is a reasonable choice of admissible functions as indicated in [1,2,3,10].

The equations of motion are derived using Lagrangian approach, which requires the computation of kinetic energy, K, and the potential energy, P, of the arm. For this arm, P is the sum of gravitational potential energy and the strain energy of the elastic links. Let the vector of generalized coordinates be $q = (\theta_1, \theta_2, q_{11}, ..., q_{1n}, q_{21}, ..., q_{2n})^T$, $\in R^{n_0}$, $n_0 = (2n+2)$. $\theta = (\theta_1, \theta_2)^T$ and $p = (q_{11}, .., q_{1n}, q_{21}, .., q_{2n})^T$ (Here T denotes transposition). Then the

Then the nonlinear equations of motion are given by

$$\frac{d}{dt}(\partial K/\partial \dot{q}_i) - (\partial K/\partial q_i) + (\partial P/\partial q_i) = B_1 u \tag{2.2}$$

where $u = (u_1, u_2)^T \in R^2$ is the vector of joint torques, q_i is the ith component of q and $B_1 = [I_{2\times 2} : O_{2\times 2n}]^T$ where I and O denote identity and null matrices of indicated dimensions. A complete derivation of the equations of motion of this arm is given in [1].

2.3 Problem formulation

We formulate the idea of controlling the links by finding the forces of torques that must be applied on the manipulator joints in order to move the links from its present position to the desired position.

For the links, the kinetic energy takes the form $K = (\dot{q}^T M(q)\dot{q}/2)$, where the inertia matrix $M(q)$ is a positive definite symmetric matrix of dimension $n_0 \times n_0$ and is a nonlinear function of q. Then (2.2)gives,

$$M(q)\ddot{q} + h_0(q, \dot{q}) + (\partial P(q)/\partial q) = B_1 u \tag{2.3}$$

where

$$h_0(q, \dot{q}) = \dot{M}\dot{q} - (1/2)\partial(\dot{q}^T M \dot{q})/\partial q$$

$$M = \begin{bmatrix} M_{11} & M_{12} \\ M_{21} & M_{22} \end{bmatrix}$$

Here M_{11} is a 2×2 matrix.

Defining the state vector $x = (q^T, \dot{q}^T)^T \in R^{2n_0}$, one can easily write (2.2) in a state variable form

$$\dot{x} = A(x) + B(x)u \tag{2.4}$$

where

$$A(x) = \begin{bmatrix} \dot{q} \\ M^{-1}(q)[-h_0(q,\dot{q}) - (\partial P(q)/\partial q)] \end{bmatrix}$$

$$B(x) = [O_{2\times n_0}, (M^{-1}(q)B_1)^T]^T$$

We assume that $(x,t) \in X[0,\infty)$ where X is a bounded open set in R^{2n_0}. We are interested in deriving a control law such that in the closed-loop system the joint angles $\theta_i(t)$, follow given reference joint angle trajectories, $\theta_{ci}(t), i = 1,2$, and the elastic oscillations caused by the manuever of the arm are stabilized. It is assumed that the reference trajectory $\theta_c(t) = (\theta_{c1}(t), \theta_{c2}(t))^T$ gives a desired path in the work space.

Let $\tilde{\theta}(t) = \theta(t) - \theta_c(t)$, $\tilde{\theta} = (\tilde{\theta_1}, \tilde{\theta_2})^T$ be the joint angle tracking error vector. Thus, (2) gives

$$\ddot{\tilde{\theta}}(t) = D_1(q)[-h(q,\dot{q})] + D_{11}(q)u - \ddot{\theta}_c(t) \tag{2.5}$$

where

$$D = [D_1^T, D_2^T]^T = M^{-1}, D_1 = [D_{11} : D_{12}], h = h_0 + (\partial P/\partial q).$$

We note that $D_{11}(q)$ is a 2×2 positive definite symmetric matrix.

In the next two chapters, we shall derive a control law based on variable struture and ultimate boundedness control theories such that $\tilde{\theta}(t) \to 0$, as $t \to \infty$

Chapter 3

Variable Structure Control

3.1 Introduction

A discontinuous joint angle control law, based on variable structure system theory, is designed which accomplishes asymptotic decoupled joint angle trajectory tracking. In the closed-loop system, the trajectories are attracted towards a chosen hypersurface in the state space and then slide along it. Although, joint angles are controlled using variable structure control (VSC) law, the flexible modes of the links are excited. Based on a linearized model about the terminal state, a stabilizer is designed using pole assignment technique to control the elastic oscillations of the links. A control logic is included which switches the stabilizer at the instant when the joint angle trajectory enters a specified neighborhood of the terminal state. Simulation results are presented to show that in the closed- loop system, accurate joint angle trajectory tracking and elastic mode stabilization are accomplished in the presence of payload uncertainty.

There are several studies related to control of rigid manipulators based on variable structure system (VSS) theory [20-28]. Using VSS theory, a discontinuous control law is obtained

which switches when the trajectory crosses a certain chosen hypersurface in the state space. The motion of the closed-loop system evolves in two phases. The first phase is the "reaching phase" in which the trajectory reaches the switching surface from any arbitrary initial condition. In the second phase, the motion is confined to the switching surface and the trajectory slides on this surface. This is termed as "sliding phase". Interestingly, the"sliding phase" is insensitive to uncertainty in the system. In view of the insensitivity of the controller to parameter changes, it is useful to extend the design approach using variable structure theory to elastic robotic systems.

In this chapter we present a design approach for the control of robotic systems with two elastic links based on VSS theory and stabilization using pole assignment. This design approach is motivated by a simple observation that the nonlinearity in the dynamics of an elastic robotic system is esssentially due to the rigid modes (joint angles), and as the time derivatives of the rigid modes vanish, the remaining motion is only due to elasticity and this is described by linear differential equations [15].

Based on VSS theory, a discontinuous control system is designed for the control of joint angles. This controller accomplishes asymptotic joint angle trajectory tracking in the closed-loop system in spite of payload uncertainty. A switching surface is chosen which is a function of the joint angle tracking error, its derivative and integral of the tracking error. Although, this integral term has not been used in [25-27], it is seen here that an improved performance is obtained when the integral term is included in the switching function. Although, the VSC law accomplishes joint angle control, it excites the elastic modes. However, interestingly, in

the closed-loop system the elastic modes are asymptotically decoupled from the rigid modes. Exploiting the asymptotic linear behavior of the closed-loop system, a stabilizer is designed using pole assignment technique for regulating the trajectory to the terminal state. In the closed-loop system, the trajectory control is achieved in two phases. In the first phase, only the VSC law is used. As the joint angle variables enter a specified neighborhood of the terminal state, a switching logic closes the stabilizer-loop, and thus in the second phase, the trajectory is controlled by the combined action of the joint angle controller and the elastic mode stabilizer.

In the next section, we shall derive a control law u_v based on VSS theory such that $\tilde{\theta}(t) \to 0$, as $t \to \infty$.

3.2 Joint Angle Control Design

Define

$$z = (\tilde{\theta}^T, \dot{\tilde{\theta}}^T)^T \tag{3.1}$$

Let $p = (p_{11}, ..., p_{1n}; p_{21}, ..., p_{2n})^T$. For the design of VSS with discontinuous control, it is essential to choose a hypersurface (switching surface) in z-space for the control function to have discontinuity, and to obtain a control law such that the trajectories of the system beginning from any initial condition are attracted towards this surface. The discontinuity surface is chosen of the form

$$S(z, z_s) = \dot{\tilde{\theta}} + 2\zeta_e \omega_{ne} \tilde{\theta} + \omega_{ne}^2 z_s \tag{3.2}$$

where $S = (s_1, s_2)^T, \zeta_e > 0, \omega_{ne} > 0$, and$z_s = (z_{s1}, z_{s2})^T$ is the integral of the tracking error satisfying,

$$\dot{z}_s = \tilde{\theta} \tag{3.3}$$

In VSS, the motion in the "sliding phase" is confined to the switching surface, i.e., $S(z, z_s) \equiv 0$. Differentiating S and using (3.3) gives,

$$\dot{S} = \ddot{\tilde{\theta}} + 2\zeta_e\omega_{ne}\dot{\tilde{\theta}} + \omega_{ne}^2\tilde{\theta} = 0 \tag{3.4}$$

We observe from (3.4), that the motion of the system is insensitive to parameter uncertainty during the sliding phase. Since the system (3.4) is asymptotically stable; $\tilde{\theta}(t) \rightarrow 0$ as $t \rightarrow \infty$, during the "sliding phase".

Now the remaining design problem in VSS is to choose u such that the trajectories of the system beginning from any initial condition move towards the switching surface. For the derivation of the control law, we use the Lyapunov approach and choose a Lyapunov function

$$V(s) = |s_1| + |s_2| \tag{3.5}$$

as suggested in[26]. We notice that the function V has discontinuity on the surface $S = 0$, and its gradient, ∇V, is not defined on $S = 0$, which forms a set of Lebesgue measure zero. The derivative of V(S) along the trajectory of the system (2.5) is given by,

$$\dot{V}(S(t)) = \xi^T \dot{S} \tag{3.6}$$

for all $\xi \in \partial V$, the generalized gradient of V (See [26] for a discussion).

To this end, it is assumed that,

$$D_{11}(q) = D_{11}^*(q) + \Delta D_{11}(q) \tag{3.7}$$

$$D_1(q)h(q,\dot{q}) = (D_1^*(q) + \Delta D_1(q))(h^*(q,\dot{q}) + \Delta h(q,\dot{q}))$$

$$\doteq D_1^*(q)h^*(q,\dot{q}) + \Delta F(q,\dot{q})$$

where, $\Delta F = D_1^*\Delta h + \Delta D_1(h^* + \Delta h)$; D_{11}^*, D_1^* and h^* are known functions; and $\Delta D_{11}, \Delta D_1$ and Δh represent the uncertainty in the robot arm dynamics. Then differentiating S and using (3.7) and (2.5) gives,

$$\dot{S} = 2\zeta_e\omega_{ne}\dot{\tilde{\theta}} + \omega_{ne}^2\tilde{\theta} - \ddot{\theta}_c - D_1^*(q)h^*(q,\dot{q}) - \Delta F(q,\dot{q}) + [D_{11}^*(q) + \Delta D_{11}(q)]u$$

$$\doteq A^*(x,t) + \Delta A^*(x) + (D_{11}^*(q) + \Delta D_{11}(q))u \tag{3.8}$$

where $\Delta A^*(x) = -\Delta F$ and

$$A^* = 2\zeta_e\omega_{ne}\dot{\tilde{\theta}} + \omega_{ne}^2\tilde{\theta} - \ddot{\theta}_c - D_1^*(q)h^*(q,\dot{q}) \tag{3.9}$$

The control law u is chosen such that $\dot{V}(t) < 0$ if $S \neq 0$. In view of (3.8), we choose u of the form,

$$u_v = (D_{11}^*(q))^{-1}[-A^*(x,t) - k\{sgn(S)\}] \tag{3.10}$$

where $k > 0$ is determined later, and

$$sgn\{S\} = [sgn(s_1), sgn(s_2)]^T$$

$$sgn\{s_i\} = \begin{cases} 1, & s_i > 0 \\ 0, & s_i = 0 \\ -1, & s_i < 0 \end{cases}$$

Substituting (3.10) in (3.8) gives,

$$\dot{S} = \Delta A^*(x) - \Delta D_{11}(q) D_{11}^{*-1}(q)\dot{(}A^*(x,t) + k\{sgn(S)\}) - k\{sgn(S)\} \tag{3.11}$$

For the nominal system when $\Delta D_1 = 0, \Delta A^* = 0$,and$\Delta D_{11} = 0$;(3.11) gives

$$\dot{S} = -k\{sgn(S)\} \tag{3.12}$$

and thus the surface $S = 0$ is reached in finite time from any initial condition satisfying $S \neq 0$.

To make $\dot{V} < 0$, in the presence of uncertainty, one needs certain bounds on the uncertain functions.

Assumption 1: Let $p(t)$ be bounded and, there exist functions $\gamma_0, \gamma_1(x)$, and γ_2 such that for each x,

$$||\Delta D_{11}(q) D_{11}^{*-1}(q)|| \leq \gamma_1(x) \leq \gamma_0 < 1 \tag{3.13}$$

$$||\Delta A^*(x) - \Delta D_{11}(q) D_{11}^{-1}(q) A^*(x,t)|| \leq \gamma_2(x,t)$$

We choose the gain k such that

$$k \geq (1 - \gamma_1(x))^{-1}(\epsilon + \gamma_2(x,t)), \epsilon > 0 \tag{3.14}$$

where ϵ is some positive real number. Now we state the following result

Theorem 1: Consider the closed-loop system (2.4),(3.3),(3.10) and (3.14). Suppose that for a given reference trajectory $\theta_c(t)$, the solution $x(t)$ beginning from initial condition $(x(t_0), t_0)$ is such that $p(t), \dot{p}(t)$, remain bounded. Then in the closed-loop system, S converges to 0 in finite time and remains zero thereafter. Thus $(\tilde{\theta}(t), \dot{\tilde{\theta}}(t)) \rightarrow 0$, as $t \rightarrow \infty$.

Proof: It can be shown following the steps of [26] that under the hypotheses of the theorem for all $S \neq 0$ and almost all $t \in [0, \infty)$

$$\dot{V}(t) \leq -\epsilon \tag{3.15}$$

and the proof is completed invoking Lyapunov stability results.

It is interesting to note that in the closed-loop system, asymptotically decoupled responses for $\tilde{\theta}_1(t)$ and $\tilde{\theta}_2(t)$ in " sliding phase" are obtained. Although, the control law u_v asymptotically follows any given $\theta_c(t)$ in spite of the presence of uncertainty in the system, elastic modes are excited.Thus it becomes necessary to design a stabilizer to damp the elastic oscillation.

The control law u_v is discontinuous and it is well known that synthesis of such a control law gives rise to chattering of trajectory about the surface $S = 0$. In order to avoid the chattering phenomenon, one uses an approximate control law which is continuous function of state [25]. An approximate control law u_{va} is obtained by replacing $sgn(S)$ by $sat(S) = (sat(s_1), sat(s_2)^T$, where

$$sat\{s_i\} = \begin{cases} 1 & s_i > \epsilon_1 \\ s_i/\epsilon_1 & |s_i| \leq \epsilon_1 \\ -1 & s_i < -\epsilon_1 \end{cases} \tag{3.16}$$

3.3 Stabilizer Design

We consider the closed loop system (2.4) with the approximate control law u_{va} given by

$$u_{va} = (D_{11}^*(q))^{-1}(-A^*(x) - k\{sat(S)\}) \tag{3.17}$$

We are interested in a stabilizer of the form

$$u_s = (D_{11}^*(q))^{-1}\omega \tag{3.18}$$

where ω is to be determined later. Thus the total control input is

$$u = u_{va} + u_s \tag{3.19}$$

For the design of stabilizer, we shall assume that there is no uncertainty in the system, i.e, $\Delta A^* = 0$ and $\Delta D_{11} = 0$. Substituting control law (3.19) in (3.8) gives ,

$$\dot{S} = -k\{sat(S)\} + \omega \tag{3.20}$$

For $\omega = 0$, it follows from (3.20) that $S(t) \rightarrow 0$, as $t \rightarrow \infty$.

We shall assume in the following that the reference trajectory $\theta_c(t)$ is such that $\theta_c(t) \rightarrow \theta^*$,a desired terminal value, $\dot{\theta}_c(t) \rightarrow 0$, $\ddot{\theta}_c(t) \rightarrow 0$, as $t \rightarrow \infty$. In the closed-loop system with control $u_{va}, \theta(t) \rightarrow \theta^*$ and $\dot{\theta}(t) \rightarrow 0$,as $t \rightarrow \infty$ and the closed-loop system gets asymptotically linearized, since nonlinearity in arm dynamics is essentially due to the joint angle variables. Thus the design of stabilizer, using linear control theory is appropriate.

We shall find it convenient to design the stabilizer in a new state space with state vector, $(\Delta\theta, S, \Delta p, \Delta\dot{p}, z_s)$, where, $\Delta\theta = \theta - \theta^*$,$\Delta p = p - p^*$. Here p^* denotes the equilibrium value of p which is obtained by solving $(q^* = (\theta^{*T}, p^{*T})^T)$

$$\partial P(q^*)/\partial p = 0 \tag{3.21}$$

Linearizing (3.20) gives,

$$\dot{S} = -(kS/\epsilon_1) + \omega \tag{3.22}$$

Assuming that $\theta_c(t)$ has converged to θ^*, one has $\tilde{\theta}(t) = \Delta\theta$. Solving for$\Delta\dot{\theta}$ from (3.2) gives,

$$\Delta\dot{\theta} = -2\zeta_e\omega_{ne}\Delta\theta + S - \omega_{ne}^2 z_s \tag{3.23}$$

Differentiating (3.23) and using (3.22) and (3.3) gives,

$$\Delta\ddot{\theta} = \omega_{ne}^2(4\zeta_e^2 - 1)\Delta\theta + (-2\zeta_e\omega_{ne} - (k/\epsilon_1))S + 2\zeta_e\omega_{ne}^3 z_s + \omega$$

Assuming that $\dot{\theta}$ is small and neglecting the second order terms, one obtains from (2.3) the following equation describing the flexible modes

$$M_{21}(q^*)\Delta\ddot{\theta} + M_{22}(p^*)\Delta\ddot{p} + P_{\theta p}(q^*)\Delta\theta + P_{pp}(q^*)\Delta p = 0 \tag{3.24}$$

where $[P_{\theta p}, P_{qp}] \doteq \partial^2 P/\partial q\partial p = [\partial^2 P/\partial\theta\partial p, \partial^2 P/\partial p\partial p]$, Using (3.24) gives

$$\Delta\ddot{p} = -M_{22}^{-1}(q^*)P_{pp}(q^*)\Delta p - M_{22}^{-1}(q^*)(M_{21}(q^*)\Delta\ddot{\theta} + P_{\theta p}(q^*)\Delta\theta) \tag{3.25}$$

Define $z = [\Delta\theta^T, S^T, \Delta p^T, \Delta\dot{p}^T, z_s^T]^T \in R^{2(n_0+1)}$. Collecting (3.3),(3.22),(3.23)and (3.25) gives

$$\dot{z} = Fz + E\omega \tag{3.26}$$

where

$$F = \begin{bmatrix} -2\xi\omega_{ne}I_{2\times2} & I_{2\times2} & O_{2\times2n} & -O_{2\times2n} & -\omega_{ne}^2 I_{2\times2} \\ 0 & -k/\epsilon_1 I_{2\times2} & 0 & 0 & 0 \\ 0 & 0 & 0 & I_{2n\times2n} & 0 \\ F_\theta & F_s & F_p & 0 & F_z \\ I_{2\times2} & 0 & 0 & 0 & 0 \end{bmatrix}$$

$$E = \begin{bmatrix} O_{2\times2} \\ I_{2\times2} \\ O_{4\times2} \\ -M_{22}^{-1}(q^*)M_{21}(q^*) \\ O_{2\times2} \end{bmatrix}$$

$$
\begin{aligned}
F_\theta &= -M_{22}^{-1}(q^*)[M_{21}(q^*)\omega_{ne}^2(4\zeta_e^2-1)+P_{p\theta}] \\
F_s &= M_{22}^{-1}(q^*)M_{21}(q^*)(2\zeta_e\omega_{ne}+(k/\epsilon_1)) \\
F_q &= -M_{22}^{-1}(q^*)P_{pp} \\
F_z &= -M_{22}^{-1}(q^*)M_{21}(q^*)2\zeta_e\omega_{ne}^3
\end{aligned}
$$

In this study, stabilizer is designed using pole assignment technique. For this purpose, a proper selection of poles of the closed-loop system is desirable. It is pointed out that once the stabilizing signal u_s is superimposed on u_{va}, the joint angle tracking ability of the control law u_{va} is affected. However, the stabilizing signal u_s is necessary for damping the elastic oscillation. Apparently, the signal u_s should be of small magnitude so that the tracking ability of u_{va} is not adversely affected, at the same time, it should be of sufficient magnitude so that rapid damping of elastic oscillation can be accomplished.

In view of (3.22),(3.23),(3.24), it easily follows that the characteristic polynomial of F is

$$
det(\lambda I - F) = (\lambda+(k/\epsilon_1))^2(\lambda^2+2\zeta_e\omega_{ne}\lambda+\omega_{ne}^2)^2.det(M_{22}(q^*)\lambda^2+P_{pp}) = 0
$$

Thus the set of eigenvalues associated with the rigid modes is $\rho_\theta = \rho_{\theta 1}\cup\rho_{\theta 2}$ where for $i=1,2$

$$
\rho_{\theta_i} = \{-k/\epsilon_1, -\zeta_e\omega_{ne} \pm j\omega_{ne}(1-\zeta_e^2)^{1/2}\}
$$

The solution of $det(M_{22}(q^*\lambda^2+P_{pp}))=0$ gives the set ρ_e of purely imaginary eigenvalues associated with the flexible modes. A good choice of closed-loop poles is the one which retains the poles ρ_θ of F associated with θ-response unaltered and shifts the imaginary poles ρ_e of F associated with the flexible modes to the left in the complex plane for stabilization.

The signal w for stabilization is of the form,

$$w = -Lz \tag{3.27}$$

Then the closed-loop system matrix is $F_{cl} = F - EL$. The complete closed-loop system is shown in Fig.2.

To this end a discussion on robustness of control law $u_{va} + u_s$ is desirable. We note that control law u_{va} for joint angle tracking is insensitive to large payload variations. The controller u_s is robust to some extent, since the complete closed-loop system is asymptotically stable. This is based on the fact that the poles of the system are continuous function of the arm parameters. However, derivation of the range of parameters for stability is an interesting but a complex problem.

3.4 Simulation Results

We present here the results of digital simulation for various initial conditions and parameters. The appendix lists the physical parameters of the flexible arm. It is assumed that the arm is initially at rest. A nominal spherical payload of mass $m_p = 4kg$ and moment of inertia $J_p = 1kgm^2$ is assumed to be attached to the end effector. The mode shapes ϕ_{ij}, are assumed to be those of a clamped-free beam.

For tracking a representative command reference trajectory is generated using a third order filter;

$$\dddot{\theta}_c + (2\zeta_c\omega_{nc} + \lambda_c)\ddot{\theta}_c + 2(\zeta_c\omega_{nc}\lambda_c + \omega_{nc}^2)\dot{\theta}_c + \omega_c^2\lambda_c\theta_c = \omega_{nc}^2\theta^*$$

such that its poles are at $-\lambda_c$ and $\{-\zeta_c\omega_{nc} \pm j\omega_{nc}(1-\zeta_c{}^2)^{1/2}\}$. The parameters chosen are $\lambda_c = 2, \zeta_c = .707, \omega_{nc} = \lambda_c/\zeta_c$ and θ^* is the terminal joint angle. Thus the poles of the command generator are at $-2, -2 \pm j2.828$. the value of ϵ_1 in (3.16) is set to 0.3. It is assumed that

$$\theta(0) = \theta_c(0) = (0,0)^T, \dot{\theta}(0) = \dot{\theta}_c(0) = 0, \theta^* = (100^0, 50^0)^T$$

Thus it is desired to track the command trajectory using control u_{va} beginning at $\theta(0)$ and terminating at θ^*. It is assumed that the elastic deflection is adequately represented by the first two modes i.e, $n = 2$, in (2.1).

Although, in the control law u_{va}, k satisfying (3.13) is used, it is appropriate to select the gain k by examining the simulated transient responses since theorem 1 gives only a sufficient condition for stability. The value of k thus selected is $k = 10$, and the feedback parameters are $\zeta_e = .707, \omega_{ne} = 3.5$. With this choice of control law u_{va},the set of poles $\rho(F)$ of F is

$$\rho(F) = \rho_\theta \cup \rho_e \tag{3.28}$$

where

$$\rho_\theta = -35., -35., -2.5 \pm j2.5, -2.5 \pm j2.5 \tag{3.29}$$

$$\rho_e = \pm j36., \pm j37., \pm j106., \pm j230$$

The feedback matrix L of the stabilizer was chosen such that the set of closed-loop poles $\rho(F_{cl})$ of the matrix F_{cl} is,

$$\rho(F_{cl}) = \rho_\theta \cup \rho_{ef} \tag{3.30}$$

where ρ_{ef}=$-.5 + re, re \in \rho_e$. It is noted that the set of eigenvalues of ρ_θ is retained in the closed-loop system and the imaginary roots of ρ_e are simply moved to the left by half unit in the complex plane. For compactness, we denote the largest joint angular velocity by $\dot{\theta}_m$ (deg/sec), the largest joint angle tracking error by $\tilde{\theta}_m$=$(\tilde{\theta}_{1m}, \tilde{\theta}_{2m})^T$ degrees,the maximum magnitude of control by $u_m = (u_{1m}, u_{2m})^T$ Nm, the elastic deflection by, $(d_{e1}, d_{e2}) = d_{e1}(L_1, t), d_{e2}(L_2, t)$ and the maximum value of elastic deflection at the tips of the links by, $d_{em} = (d_{e1m}, d_{e2m})$.

3.4.1 Trajectory Control : Stabilizer loop open

In order to observe the behavior of the closed loop system (2.4),(3.3),(3.17) to the control input u_{va}, the system was simulated without the stabilizer. Selected response plots are shown in Fig 3. As expected, for this nominal case, the tracking error $\tilde{\theta}(t)$ was identically zero. The response time of θ was nearly 3 seconds. The manuever of the arm resulted in the excitation of the elastic modes and figure shows persistent periodic oscillations of the elastic modes. The maximum values were: $\dot{\theta}_m = (83.5, 42.5)$ deg/sec, $d_{em} = (.057, .029)$ meter and, $u_m = (227, 86.5) Nm$.

3.4.2 Trajectory Control : Stabilizer loop closed

Nominal Load

The complete closed-loop system (2.4),(3.3),(3.17) and(3.18) including the stabilizer (3.27) was simulated with a nominal payload with zero initial conditions of joint angles. The selected responses are shown in fig 4. Notice that the switching logic closes the stabilizer

loop in about 5 seconds when the trajectory enters the vicinity of terminal value. The instant of switching of the stabilizer was selected by examining the θ-responses in case (3.4.1). The tracking error $\tilde{\theta}$ is identically zero before the closing of the stabilizer in the feedback loop. However a small transient in the θ- response is caused when the stabilizer was included in the loop, but the tracking error is quite small. It is seen that the system settles to steady state within 2.5 seconds after the stabilizer loop was closed. The maximum values were: $\dot{\theta}_m = (83.5, 42)$ deg/sec, $u_m = (225, 86)$ Nm, $\tilde{\theta}_m = (1.35, .22)$ deg and $d_{em} = (.057, .026)$ meter.

Initial tracking error

Simulation was carried out with a nonzero initial condition of $\theta(0) = (10^0, 5^0)^T$ giving an initial tracking error of $\tilde{\theta}(0) = (10^0, 5^0)^T$. The control parameters, and command trajectory of the nominal case were retained. As expected, larger control torque is required due to nonzero initial tracking error and also larger elastic deflection is caused (see Fig.5). The maximum values were: $\dot{\theta}_m = (88.5, 42.6)$ deg/sec, $u_m = (600, 230)$ Nm, $\tilde{\theta}_m = (8.8, 4.3)$ deg, and $d_{em} = (.125, .075)$ meter.

Lower Payload

The simulation was carried out with a perturbed payload of mass $m_p = 2kg$ and $J_p = .5kgm^2$ which is 50 % lower than the nominal payload. However, the controller which was designed for the nominal parameters was retained. Fig 6, shows the insignificant effect of change of

payload on responses. The elastic deflection is smaller than that of the nominal case. The control torque is also less compared to the nominal case due to the reduced payload. The maximum values were: $\dot{\theta}_m = (83.5, 41)$ deg/sec, $u_m = (217, 52)$ Nm, $\tilde{\theta}_m = (0.48, .68)$ deg and $d_{em} = (.052, .013)$ meter.

Higher payload

The payload mass m_p was increased to $6kg$ and J_p was increased to $1.5kgm^2$ giving an increase of 50% in nominal payload mass and inertia. However, the controller designed for the nominal payload was used in simulation. Accurate trajectory tracking and rapid stabilization of elastic modes were observed (see Fig.7). However, larger torque is required. This is expected since the payload has increased. The maximum values were: $\dot{\theta}_m = (84.5, 43.5)$ deg/sec, $u_m = (260, 120)$ Nm, $\tilde{\theta}_m = (0.25, .56)$ deg and $d_{em} = (.058, .036)$ meter.

Insensitivity of stabilizer to θ^*

In order to examine the sensitivity of the stabilizer gain matrix L, control of arm to different terminal joint angles $\theta^* = (140^0, 70^0)^T$ and $\theta^* = (80^0, 40^0)$, were tried. However the stabilizer designed for $\theta^* = (100^0, 50^*)$ with the nominal payload was retained in simulation. Smooth θ-responses and elastic mode stabilization were obtained. These results showed that the stabilizer is robust to perturbation in θ^* and, therefore the, same stabilizer gain matrix L can be used for controlling the arm in a neighbourhood of a nominal terminal θ^*. The maximum values were: $\dot{\theta}_m = (116, 58.5)$ deg/sec, $u_m = (230, 120)$ Nm, $\tilde{\theta}_m = (.55, .95)$

deg and $d_{em} = (-.053, .02)$ meter for the terminal command of $\theta^* = (140, 70)$ deg., and $\dot{\theta}_m = (66, 34)$ deg/sec, $u_m = (225, 75)$ Nm, $\tilde{\theta}_m = (.18, .7)$ deg and $d_{em} = (.057, .024)$ meter, for the terminal command of $\theta^* = (80, 40)$ deg.

3.5 Conclusion

A design approach for the control of a flexible robotic arm based on VSS theory and pole assignment technique for stabilization was presented. The joint-angle controller was designed based on VSS theory to obtain independent control of joint angles. An integral feedback of tracking error was used in the VSC law to obtain improved performance. A stabilizer was designed to damp the elastic vibration caused due to the movement of the arm. In the closed-loop system, the system trajectory evolves in two phases. In the first phase, joint angles are controlled along prescribed path and in the second phase a switching logic closes the stabilizer when the joint angle tracking error reaches the vicinity of the terminal state. The closed-loop system is robust to uncertainty in the payload. Simulation results showed that the closed-loop system can achieve accurate trajectory tracking and elastic mode stabilization.

Chapter 4

Ultimate Boundedness Control

4.1 Introduction

In this chapter we present a design approach for the control of robotic systems with two elastic links based on the theory of ultimate boundedness and stabilization using the pole assignment technique. A nonlinear continuous control law is derived such that in the closed-loop system the joint angle tracking error is uniformly ultimately bounded [23-25]. Furthermore, joint angle trajectory error dynamics are asymptotically decoupled in an appropriate sense. The joint angle controller includes a reference trajectory generator and integral tracking error feedback. The additional integral feedback gives improved performance as seen in [25]. Although, the UBC accomplishes joint angle control, it excites the elastic modes of the links. Exploiting the asymptotic linear behavior of the closed-loop system, a stabilizer is designed using pole assignment technique for regulating the trajectory to the terminal state. In the closed-loop system, the trajectory control is achieved in two phases. In the first phase, only the nonlinear joint angle controller is used. As the joint angle variables enter a specified neighborhood of the terminal state, a switching logic closes the stabilizer-loop, and thus

in the second phase, the trajectory is controlled by the combined action of the joint angle controller and the stabilizer.

For the synthesis of the control law, it is assumed that all the state variables are available for feedback. In a practical situation one has to obtain the estimate of states using an observer and sensors (strain gages, optical devices and accelerometers, etc.,). One can use strain gages to obtain the elastic modes as in [10] and filters can be used to get an estimate of modal velocity.

4.2 Joint Angle Control Design

For the design of a joint angle controller, it is assumed that the parameters of the arm are not precisely known. In view of (2.5), let

$$\ddot{\tilde{\theta}}(t) = -D_1^*(q)h^*(q,\dot{q}) - \ddot{\theta}_c(t) + [D_{11}^*(q) + \Delta D_{11}(q)]u - D_1^*(q)\Delta h(q,\dot{q}) - \Delta D_1(q)h^*(q,\dot{q}) \quad (4.1)$$

where D_1^*, h^* and D_{11}^* denote the known functions and ΔD_1, Δh, and ΔD_{11} are the uncertain matrices such that $D_1 = D_1^* + \Delta D_1$, $h = h^* + \Delta h$, and $D_{11} = D_{11}^* + \Delta D_{11}$.

We choose a control law of the form

$$u_u = {D_{11}^*}^{-1}(q)[D_1^*(q)h^*(q,q^*) + \ddot{\theta}_c(t) - K_2\dot{\tilde{\theta}} - K_1\tilde{\theta} - K_0 z_s + u_r] \quad (4.2)$$

$$\doteq f(x, z_s, t) + {D_{11}^*}^{-1}(q)u_r$$

where K_j =diag(k_{ij}), $j = 0,1,2$, $i = 1,2$, are constant feedback gains, u_r is an additional control signal to be determined later for robustness, and $z_s = (z_{s1}, z_{s2})^T \in N$, a bounded,

open set in R^2, satisfies

$$\dot{z}_s = \tilde{\theta} \tag{4.3}$$

In the closed-loop system (2.4) and (4.2) when $\Delta D_1 = 0$, $\Delta D_{11} = 0$ and $\Delta h = 0$, one has

$$\ddot{\tilde{\theta}} + K_2\dot{\tilde{\theta}} + K_1\tilde{\theta} + K_0 z_s = 0 \tag{4.4}$$

and decoupled responses for $\theta_i(t)$ are obtained. However, in the presence of uncertainty additional coupling terms appear in (4.4). Now a control signal u_r will be derived to compensate for the uncertainty such that $(\tilde{\theta}, \dot{\tilde{\theta}})$ trajectory is uniformly ultimately bounded.

Let $z = (z_1^T, z_2^T)^T$, $z_i = (\tilde{\theta}_i, \dot{\tilde{\theta}}_i, z_{si})^T$, $i = 1,2$ and $z \in M_0$ for all $(x, z_s) \in X \times N$. Then the differential equation for z can be written as

$$\dot{z} = Ez + Fw \tag{4.5}$$

where E =diag(E_i), F =diag(F_i), $i = 1,2$; $F_i = [0,1,0]^T$, $w = -D_1^*(q)\Delta h(q,\dot{q})$
$- \Delta D_1(q)h(q,\dot{q}) + \Delta D_{11}(q)[f(x,z_s,t) + (D_{11}^*(q))^{-1}u_r] + u_r$ and

$$E_i = \begin{bmatrix} 0 & 1 & 0 \\ -k_{i1} & -k_{i2} & -k_{i0} \\ 1 & 0 & 0 \end{bmatrix}$$

The matrices K_i are chosen such that E is a Hurwitz matrix. Thus given any positive definite symmetric matrix Q =diag(Q_{ii}), $i = 1,2$, (denoted as $Q > 0$) there exists a unique solution $R > 0 (R = diag(R_{ii}), i = 1,2)$ of the Lyapunov equation

$$E^T R + RE = -Q \tag{4.6}$$

Define $v = (v_1, v_2)^T = F^T Rz$, and $v_i = F_i^T R_{ii} z_i, i = 1,2$.

To this end, it is esential to obtain certain bounds on uncertain functions. Define

$\alpha(x, z_s, t) = -D_1^*(q)\Delta h(q, \dot{q}) - \Delta D_1(q)h(q, \dot{q}) + \Delta D_{11}(q)f(x, z_s, t)$

Assumption 1 : There exist functions β_i, γ_i, $i = 1, 2$, and constants γ_0 and β_{20} such that for $(x, t) \in M$, $z_s \in N$,

$$\| \Delta D_{11}(q) {D_{11}^*}^{-1}(q) \| \leq \gamma_1(q) < \gamma_0 < 1 \tag{4.7}$$

$$\| \alpha(x, z_s, t) \| \leq \beta_1(x, z_s, t) \leq \beta_{20}$$

$$\| (F^T R F)^{-1} F^T R E z + \alpha(x, z_s, t) \| \leq \beta_1(x, z_s, t)$$

$$\gamma_2(x, z_s, t) = sup[\beta_1(x, z_s, t), \beta_2(x, z_s, t), (x, t) \in M, z_s \in N]$$

Now we consider a class of control laws of the form

$$u_r = -K(x, z_s, t)v/(\| v \| + \delta) \tag{4.8}$$

where the gain $K(x, z_s, t)$ is to be determined later and δ is a small positive number. Let $\varepsilon > 0$ be a given positive number. Define ellipsoids as

$$Z(r) = \{z \in R^6 : z^T P z \leq r > 0\}$$

Now let

$$r^* = min\{r : Z(r) \supseteq B(\eta)\} \tag{4.9}$$

where ($\lambda_m(Q)$ denotes the minimum eigenvalue of Q)

$$\eta = [2\beta_{20}\delta\{2\delta + \varepsilon - 2(\delta^2 + \varepsilon\delta)^{1/2}\}/(\varepsilon\lambda_m(Q))]^{1/2} \tag{4.10}$$

$$B(\eta) = \{z \in R^6 : \| z \| \leq \eta\}$$

Thus $Z(r^*)$ is the smallest ellipsoid which contains the ball $B(\eta)$ and $r^* = \lambda_M(P)\eta^2$, where $\lambda_M(P)$ is the largest eigenvalue of P. Consider also ellipsoids $Z(r_1)$ with $r_1 > r^*$ and $Z(r_0)$ with $r_0 = z_0^T R z_0, z_0 = z(t_0)$.

Now suppose that $K(x, z, t)$ is selected such that

$$K(x, z, t) > \gamma_2(x, z, t)(\varepsilon + \delta)/\{\varepsilon(1 - \gamma_1(x, t))\} \tag{4.11}$$

Then the following result can be stated.

Theorem : Consider system (2.1), (4.2), (4.3), (4.8), and (4.11) with control law $u = u_u$. Suppose that in the closed-loop system, the trajectory $x(t)$ beginning at $(x_0, t_0) \in M$ remains in X and $z_s \in N$ for all $t \geq t_0$, and $Z(r_0) \subset M_0$. Then the trajectory of the closed-loop system enters the set $\Omega = Z(r_1) \bigcap S(\varepsilon_1)$ for any $r_1 > r^*$ and $\varepsilon_1 > \varepsilon$,where

$$S(\varepsilon_1) = \{z \in R^6 : \| F^T R z \| \leq \varepsilon_1\}$$

in a finite time (which depends on z_0) and remains in it thereafter.

Proof : For showing ultimate boundedness of trajectory in the set $Z(r_1)$ one chooses a Lyapunov function $W(z) = z^T R z$, and shows that $\dot{W} < 0$ if $z \notin B(\eta)$. Furthermore, uniform attractivity of $S(\varepsilon_1)$ is proved by showing that $\dot{H}(v) < 0$ for $\| v \| > \varepsilon$ where $H(v) = v^T (F^T R F)^{-1} v$. Since the proof can be completed following the arguments of [24-25], the details are not given here.

According to the theorem, the motion of the closed-loop system is uniformly ultimately bounded, that is, the trajectory error $\tilde{\theta}$ is such that $z(t) \in Z(r_1)$, the set of ultimate bound-

edness, after a finite interval of time. In fact $z(t)$ is confined in the neighborhood of the hyperplane $v = 0$ after a finite time. The size of the set of ultimate boundedness can be reduced by taking smaller value of δ, since in view of (4.10), $\eta \rightarrow 0$ as $\delta \rightarrow 0$. However, for extremely small values of δ , the digital implementation of the control law may lead to control chattering. On the other hand, large values of δ may cause unacceptable tracking error. Therefore, a compromise must be made in the choice of δ. In the closed-loop system the joint angle tracking error is uniformly ultimately bounded.

However, the maneuver of the arm excites the elastic modes of the links and it becomes necessary to damp the elastic oscillation.

4.3 Stabilizer Design

We shall assume in the following that the reference trajectory $\theta_c(t)$ is such that $\theta_c(t) \rightarrow \theta^*$, a desired terminal value, $\dot{\theta}_c(t) \rightarrow 0$, $\ddot{\theta}_c(t) \rightarrow 0$, as $t \rightarrow \infty$. In the closed-loop system with control u_u, the trajectory $(\tilde{\theta}, \dot{\tilde{\theta}})$ is uniformly ultimately bounded, and tends to a small neighborhood of $(\tilde{\theta} = 0, \dot{\tilde{\theta}} = 0)$. We note that the closed-loop system gets asymptotically linearized, since nonlinearity in arm dynamics is essentially due to the joint angle variables. Thus the design of stabilizer, using linear control theory is appropriate.

In order to stabilize the elastic modes, an additional signal is superimposed on the control law u_u at t_s ; where t_s is the instant where the trajectory $(\theta, \dot{\theta})$ enters a small neighborhood of $(\theta^*, 0)$. Let the complete control signal be $u = u_u + u_s$. The stabilizing signal u_s is derived based on a linearized model of the arm about the terminal state. However, in order to design

the stabilizer, it is assumed in the following that there is no uncertainty in the system.

Let the equilibrium point of the system be $q^* = (\theta^{*T}, p^{*T})$ where p^* is the solution of

$$\partial P(q^*)/\partial p = 0 \tag{4.12}$$

For simplicity, we select $Q_{ii} = I_{3\times3}$ (a 3×3 identity matrix). Let $R_{ii} = (r_{jk})$, $j,k = 1,2,3$ and $i = 1,2$ Then it is easily seen that

$$v_i = r_{12}\tilde{\theta}_i + r_{22}\dot{\tilde{\theta}}_i + r_{23}z_{si}, i = 1,2 \tag{4.13}$$

We shall choose the stabilizing signal as $u_s = D_{11}^{*-1}(q)w_s$. For the design of stabilizer, we set the gain in (4.8) as K^*, a constant, for $t \geq t_s$, the switching instant, where $K^* \geq K(x(t_s),z_s(t_s),t_s)$. Then for the nominal system, it follows from (4.1), (4.2), and (4.8) that

$$\ddot{\tilde{\theta}} = -K_2\dot{\tilde{\theta}} - K_1\tilde{\theta} - K_0z_s - K^*v/(\| v \| +\delta) + w_s \tag{4.14}$$

Let $\Delta\theta = (\theta - \theta^*)$ and $\Delta p = p - p^*$. Linearizing (4.14) and noting that $\tilde{\theta} \approx \Delta\theta$ for large t, one has

$$\Delta\ddot{\tilde{\theta}} = -K_2\Delta\dot{\theta} - K_1\Delta\theta - K_0z_s - K^*v/\delta + w_s \tag{4.15}$$

$$= (-\frac{K^*}{\delta}r_{22}I - K_2)\Delta\dot{\theta} + (-\frac{K^*}{\delta}r_{12}I - K_1)\Delta\theta + (-\frac{K^*}{\delta}r_{23}I - K_0)z_s + w_s$$

$$\doteq K_{2a}\Delta\dot{\theta} + K_{1a}\Delta\theta + K_{0a}z_s + w_s$$

Assuming that $\dot{\theta}$ is small and neglecting the second order terms, one obtains from (2.3) the following equation describing the flexible modes

$$M_{21}(q^*)\Delta\ddot{\tilde{\theta}} + M_{22}(q^*)\Delta\ddot{\tilde{p}} + P_{\theta p}(q^*)\Delta\theta + P_{pp}(q^*)\Delta p = 0 \tag{4.16}$$

where

$[P_{\theta p}, P_{qp}] \doteq \partial^2 P/\partial q \partial p = [\partial^2 P/\partial\theta\partial p, \partial^2 P/\partial p \partial p]$, Using (4.15) in (4.16), gives

$$\Delta\ddot{p} = -M_{22}^{-1}(q^*)P_{pp}(q^*)\Delta p - M_{22}^{-1}(q^*)(M_{21}(q^*)\Delta\ddot{\theta} + P_{\theta p}(q^*)\Delta\theta) \tag{4.17}$$

Define $x_a = [\Delta\theta^T, \Delta\dot{\theta}, \Delta p^T, \Delta\dot{p}^T, z_s^T]^T \in R^{2(n_0+1)}$. Collecting (4.3),(4.15), and (4.17) gives

$$\dot{x}_a = F_a x_a + E_a w_s \tag{4.18}$$

where

$$F_a = \begin{bmatrix} 0_{2\times2} & I_{2\times2} & O_{2\times2n} & O_{2\times2n} & 0_{2\times2} \\ K_{1a}I_{2\times2} & K_{2a}I_{2\times2} & 0_{2\times2n} & 0_{2\times2n} & K_{0a}I_{2\times2} \\ 0_{2n\times2} & 0_{2n\times2} & 0_{2n\times2n} & I_{2n\times2n} & 0_{2n\times2} \\ \tilde{F}_1 & F_2 & F_p & 0_{2n\times2n} & F_0 \\ I_{2\times2} & 0_{2\times2} & 0_{2\times2n} & 0_{2\times2n} & 0_{2\times2} \end{bmatrix}$$

$$E_a = \begin{bmatrix} O_{2\times2} \\ I_{2\times2} \\ O_{2n\times2} \\ -M_{22}^{-1}(q^*)M_{21}(q^*) \\ O_{2\times2} \end{bmatrix}$$

$$F_i = -M_{22}^{-1}(q^*)M_{21}(q^*)K_{ia}, i = 0,1,2$$

$$\tilde{F}_1 = F_1 - M_{22}^{-1}(q^*)P_{\theta p}(q^*)$$

$$F_p = -M_{22}^{-1}(q^*)P_{pp}$$

In this study, stabilizer is designed using pole assignment technique. For this purpose, a proper selection of poles of the closed-loop system is desirable. It is pointed out that once the stabilizing signal u_s is superimposed on u_u, the joint angle tracking ability of the control law u_u is affected. However, the stabilizing signal u_s is necessary for damping the elastic

oscillation. Apparently, the signal u_s should be of small magnitude so that the tracking ability of u_u is not adversely affected, at the same time, it should be of sufficient magnitude so that rapid damping of elastic oscillation can be accomplished.

In view of (4.15), (4.17), it easily follows that the characteristic polynomial of F_a is

$$det(\lambda I - F_a) = det(\lambda^3 I_{2\times 2} + K_{2a}\lambda^2 + K_{1a}\lambda + K_{0a}).det(M_{22}(q^*)\lambda^2 + P_{pp}) = 0$$

Thus the set of eigenvalues associated with the rigid modes is ρ_θ which is obtained by solving $det(\lambda^3 I_{2\times 2} + K_{2a}\lambda^2 + K_{1a}\lambda + K_{0a}) = 0$.

The solution of $det(M_{22}(q^*\lambda^2 + P_{pp})) = 0$ gives the set ρ_e of purely imaginary eigenvalues associated with the flexible modes. A good choice of closed-loop poles is the one which retains the poles ρ_θ of F_a associated with θ-response unaltered and shifts the imaginary poles ρ_e of F_a associated with the flexible modes to the left in the complex plane for stabilization. The signal w_s for stabilization is of the form,

$$w_s = -Lx_a \tag{4.19}$$

Then the closed-loop system matrix is $F_{cl} = F_a - E_a L$. The complete closed-loop system is shown in Fig.2.

To this end a discussion on robustness of control law $u_u + u_s$ is desirable. We note that control law u_u for joint angle tracking is insensitive to large payload variations. The controller u_s is robust to some extent, since the complete closed-loop system is asymptotically stable. This is based on the fact that the poles of the system are continuous function of the arm

parameters. However, derivation of the range of parameters for stability is an interesting but a complex problem.

4.4 Simulation Results

We present here the results of digital simulation for various initial conditions and parameters. The appendix lists the physical parameters of the flexible arm. It is assumed that the arm is initially at rest. A nominal spherical payload of mass $m_p = 4kg$ and moment of inertia $J_p = 1kgm^2$ is assumed to be attached to the end effector. The mode shapes ϕ_{ij}, are assumed to be those of a clamped-free beam.

For tracking a representative command reference trajectory is generated using a third order filter;

$$\dddot{\theta}_c + (2\zeta_c\omega_{nc} + \lambda_c)\ddot{\theta}_c + 2(\zeta_c\omega_{nc}\lambda_c + \omega_{nc}^2)\dot{\theta}_c + \omega_c^2\lambda_c\theta_c = \omega_{nc}^2\theta^*$$

such that its poles are at $-\lambda_c$ and $\{-\zeta_c\omega_{nc} \pm j\omega_{nc}(1-\zeta_c{}^2)^{1/2}\}$. The parameters chosen are $\lambda_c = 2, \zeta_c = .707, \omega_{nc} = \lambda_c/\zeta_c$ and θ^* is the terminal joint angle. Thus the poles of the command generator are at $-2, -2 \pm j2.828$. the value of δ in (4.14) is set to 0.5. It is assumed that

$$\theta(0) = \theta_c(0) = (0,0)^T, \dot{\theta}(0) = \dot{\theta}_c(0) = 0, \theta^* = (100^0, 50^0)^T$$

Thus it is desired to track the command trajectory beginning at $\theta(0)$ and terminating at θ^*. It is assumed that the elastic deflection is adequately represented by the first two modes i.e, $n = 2$, in (2.1).

Although, in the control law u_u, K satisfying (4.11) is used, it is appropriate to select the gain K by examining the simulated transient responses since Theorem 1 gives only a sufficient condition for uniform ultimate boundedness. The value of K thus selected is $K = K^* = 20$. The feedback gains k_{ij} were set to $k_{i0} = 700.$, $k_{i1} = 200.$ and $k_{i2} = 21$, $i = 1, 2$. With this choice of control law u_u, the set of poles $\rho(F_a)$ of F_a is

$$\rho(F_a) = \rho_\theta \cup \rho_e \tag{4.20}$$

where

$$\rho_\theta = \{-6.95, -6.95, -7.04 \pm j7.05, -7.04 \pm j7.05\} \tag{4.21}$$

$$\rho_e = \{\pm j36.58, \pm j37.2, \pm j106.4, \pm j230.\}$$

The feedback matrix L of the stabilizer was chosen such that the set of closed-loop poles $\rho(F_{cl})$ of the matrix F_{cl} is,

$$\rho(F_{cl}) = \rho_\theta \cup \rho_{ef} \tag{4.22}$$

where ρ_{ef}=$-1. + re, re \in \rho_e$. It is noted that the set of eigenvalues of ρ_θ is retained in the closed-loop system and the imaginary roots of ρ_e are simply moved to the left by half unit in the complex plane. For compactness, we denote the largest joint angular velocity by $\dot{\theta}_m$ (deg/sec), the largest joint angle tracking error by $\tilde{\theta}_m$=$(\tilde{\theta}_{1m}, \tilde{\theta}_{2m})^T$ degrees,the maximum magnitude of control by $u_m = (u_{1m}, u_{2m})^T$ Nm, the elastic deflection by, $(d_{e1}, d_{e2}) = \delta_1(L_1, t), \delta_2(L_2, t)$ and the maximum value of elastic deflection at the tips of the links by, $d_{em} = (d_{e1m}, d_{e2m})$.

4.4.1 Trajectory Control : Stabilizer loop open

In order to observe the behavior of the nominal closed loop system (2.4),(4.2),(4.3) with the nominal control input u_u, the system was simulated without the stabilizer. Selected response plots are shown in Fig. 9. As expected, for this nominal case, the tracking error $\tilde{\theta}(t)$ was identically zero. The response time of θ was nearly 2.5 seconds. The manuever of the arm resulted in the excitation of the elastic modes and figure shows persistent periodic oscillations of the elastic modes. The maximum values were: $\dot{\theta}_m = (83., 42.)$ deg/sec, $d_{em} = (.052, .026)$ meter and, $u_m = (232, 88.2)Nm$.

4.4.2 Trajectory Control : Stabilizer loop closed

Nominal load

The complete closed-loop system (2.4),(4.2),(4.3), and(4.19) including the stabilizer was simulated with a nominal payload. The selected responses are shown in Fig. 10. Notice that the switching logic closes the stabilizer loop in about 3 seconds when the trajectory enters the vicinity of terminal value. The instant of switching of the stabilizer was selected by examining the θ-responses in case of nominal open loop. The tracking error $\tilde{\theta}$ is identically zero before the closing of the stabilizer in the feedback loop. However a small transient in the θ- response is caused when the stabilizer was included in the loop, but the tracking error is quite small. It is seen that the system settles to steady state within 3.5 seconds after the stabilizer loop was closed. The maximum values were: $\dot{\theta}_m = (82.2, 41.3)$ deg/sec, $u_m = (235, 87)$ Nm, $\tilde{\theta}_m = (.35, 1.85)$ deg and $d_{em} = (.0535, .0265)$ meter.

Initial tracking error

Simulation was carried out with a nonzero initial condition of $\theta(0) = (15^0, 5^0)^T$ giving an initial tracking error of $\tilde{\theta}(0) = (15^0, 5^0)^T$. However, the control parameters, and command trajectory of the nominal case were retained. As expected, larger control torque is required due to nonzero initial tracking error and also larger elastic deflection is caused (Fig. 11) The maximum values were: $\dot{\theta}_m = (88.3, 182.6)$ deg/sec, $u_m = (1500, 730)$ Nm, $\tilde{\theta}_m = (15., 16.2)$deg, and $d_{em} = (.325, .215)$ meter.

Lower Payload

The simulation was carried out with a perturbed payload of mass $m_p = 2kg$ and $J_p = .5kgm^2$ which is 50 % lower than the nominal payload. However, the zero initial conditions and the controller designed for the nominal parameters were retained. Fig. 12 shows the insignificant effect of change of payload on responses. The elastic deflection is smaller than that of the nominal case. The control torque is also less compared to the nominal case due to the reduced payload. The maximum values were : $\dot{\theta}_m = (84.5, 40.4)$ deg/sec, $u_m = (187, 47)$ Nm, $\tilde{\theta}_m = (0.26, .78)$ deg and $d_{em} = (.0475, .0132)$ meter.

Higher payload

The payload mass m_p was increased to $6kg$ and J_p was increased to $1.5kgm^2$ giving an increase of 50% in nominal payload mass and inertia. However, the controller designed for the nominal payload and zero initial conditions of nominal load case were used in simulation.

Accurate trajectory tracking and rapid stabilization of elastic modes were observed, Fig.13. However, larger torque compared to that of nominal load is required. This is expected since the payload has increased. The maximum values were: $\dot{\theta}_m = (84.25, 42.5)$ deg/sec, $u_m = (255, 122)$ Nm, $\tilde{\theta}_m = (0.46, .95)$ deg and $d_{em} = (.0574, .0365)$ meter.

Insensitivity of stabilizer to θ^*

In order to examine the sensitivity of the stabilizer gain matrix L, control of arm to different terminal joint angles $\theta^* = (120^0, 40^0)^T$), were tried. However the stabilizer designed for $\theta^* = (100^0, 50^0)$ with the nominal payload was retained in simulation. Smooth θ-responses and elastic mode stabilization were obtained (see Fig 14). These results showed that the stabilizer is robust to perturbation in θ^* and, therefore the, same stabilizer gain matrix L can be used for controlling the arm in a neighbourhood of a nominal terminal θ^*. The maximum values were: $\dot{\theta}_m = (100., 33.5)$ deg/sec, $u_m = (230, 120)$ Nm, $\tilde{\theta}_m = (.53, 2.35)$ deg and $d_{em} = (.0525, .029)$ meter for the terminal command of $\theta^* = (120, 40)$ deg.

4.5 Conclusion

A design approach for the control of a flexible robotic arm based on the theory of Ultimate boundedness and pole assignment technique for stabilization was presented. The UBC was designed for the control of joint angles. An integral feedback of tracking error was used in the UBC to obtain improved performance. A stabilizer was designed to damp the elastic vibration caused by the movement of the arm. In the closed-loop system, the system tra-

jectory evolves in two phases. In the first phase, joint angles are controlled along prescribed paths and in the second phase a switching logic closes the stabilizer when the joint angle tracking error reaches the vicinity of the terminal state. The closed-loop system is robust to uncertainty in the payload. Simulation results showed that the closed-loop system can achieve accurate trajectory tracking and elastic mode stabilization.

Chapter 5

Implementation of Variable Structure Control Law

5.1 Introduction

We consider control of an elastic robotic arm via a Digital Signal Processor(DSP). The control law based on Variable Structure System theory is designed so as to accomplish asymptotic joint angle trajectory tracking of single link manipulator. The DSP used in this research is TMS320C25 from Texas Instruments which has superior performance over its competitors in terms of its high-speed execution capability. This is one of the main requirements of implementation of real-time digital controls. The experimental set up consists of a Direct Current (DC) motor of Permanent Magnetic field with a Tacho Generator, a Power Amplifier to drive the motor and a feedback potentiometer mounted on the front end of the shaft. A manipulator arm of one inch width and one meter length is attached to the shaft of the motor. The motor is mounted on a rigid frame and interfaced to the DSP via a suitable signal conditioner. The DSP itself is housed in the IBM Personal Computer for inputting data and command which is being supported by the CHIMERA development system of

Atlanta Signal Processors, Inc.

Introduction of microprocessors and, more recently, signal processors has radically altered the field of high performance servo control over the past decade. The advent of digital techniques has presented the designer with tremendous flexibility in control algorithm design. However, this migration from analog to digital has several problems associated with it. In particular, the design of the digital control algorithm must take account of the sampled data nature of the system. Problem due to the delays introduced by the sampling period, and the computation time must be carefully considered in the design of feedback parameters. The quantization noise due to the digital nature of the position information must also be carefully analyzed and its effects minimized. The TMS320C25 DSP has a 16×16 multiplier, scaling shifter and stack whose functions are of hardware in nature, thus the speed of operation is much higher than conventional microprocessors. Further, the device employs a dual-bus Harvard architecture with single-cycle execution of most instructions. This hardware-intensive approach provides computing power previously unavailable on a single chip. It has on chip RAM and ROM and can address a total of 64K words of data memory .

5.2 The Experiment

Here we consider control of a robotic arm with one link. The schematic diagram of the digital control scheme is shown in figure 14. The experimental setup is shown in Figure 15. The DC servo motor produces the torque necessary to control the joint angle of the robot arm. The potentiometer and the tachometer out puts are taken as position and velocity feedbacks

and applied to DSP through a 16 bit analog-to-digital converters. The sampling period is programmed to 2000 samples per second.

It is assumed that the arm is initially at rest. For tracking a representative command, a reference trajectory is generated using a second-order system described by

$$\frac{\theta_c(s)}{\theta^*(s)} = \frac{\omega_c^2}{s^2 + 2\zeta_c\omega_c s + \omega_c^2} \tag{5.1}$$

or equivalently in time domain,

$$\ddot{\theta}_c + 2\zeta_c\omega_c\dot{\theta}_c + \omega_c^2\theta_c = \omega_c^2\theta^*$$

where $\zeta_c = 0.707, \omega_c = 1$, and θ^* is the desired terminal joint angle. The second-order system can be expressed in z transform as

$$\frac{\theta_c(z)}{\theta^*(z)} = \frac{y(z)}{x(z)} = \frac{b_1 z^{-1} + b_2 z^{-2}}{1 - a_1 z^{-1} + a_2 z^{-2}} \tag{5.2}$$

taking inverse z transform we obtain the difference equation of the trajectory

$y(nT) = b_1 x[(n-1)T] + b_2 x[(n-2)T] + a_1 y[(n-1)T]$

$-a_2 y[(n-2)T]$

both $y(nT)$ and $x(nT)$ are zero for $n \leq 0$, for $n \geq 2$ the above equation becomes

$$y(nT) = b_0 x_{nT} + a_1 y[(n-1)T] - a_2 y[(n-2)T] \tag{5.3}$$

where $x(nT)$ is the unit step and the coefficients a_1, a_2 and b_0 are suitably selected for smooth response. The typical values of a_1, a_2 and b_0 are 1, 0.005 and 0.005, respectively for typical response time of 2 seconds. Here the trajectory command is y(nT), the derivative of trajectory is $[y(nT) - y(n-1)T]/T$ and sampling period is T.

The difference equation of hyper surface as given by (3.2) is

$$S(nT) = 2\zeta_e\omega_e[\theta(nT) - \theta_c(nT)] + [\dot{\theta}(nT) - \dot{\theta}_c(nT)] + \omega_e^2 r_s(nT) \tag{5.4}$$

which can be written as

$$S(n) = k_p e_p(n) + k_d e_v(n) + k_i r(n) \tag{5.5}$$

where

$$e_p(n) = y(n) - f_p(n) \tag{5.6}$$

$$e_v(n) = (y(n) - y(n-1)) - f_v(n) \tag{5.7}$$

$$r(n) = b'(e_p(n) + e_p(n-1)) + a' r(n-1) \tag{5.8}$$

In the above expressions; f_p and f_v are the position and velocity feedbacks; the coefficients k_p, k_d and k_i are the proportional, derivative and integral constants, taken to be $k_p = 2\zeta_e\omega_e$, $k_d = 1$ and $k_i = \omega_e^2$ where $\omega_e = \lambda/\zeta_e$. The typical value of $\lambda = 0.5$ and $\zeta = 0.707$ for a stable response. For critical response we choose $\lambda = 0.707$ such that the poles are at $-0.707 \pm j0.707$, $e_p(n)$ and $e_v(n)$ are the position and velocity errors; the b', a' are the coefficients of the trapezoidal integrator of the integral feedback where $a' = 1$ and $b' = T/2$

.

The signal S is then applied to the $sgn\{S\}$ function to check for the sign. After comparison, a value, either $-K$ or a $+K$ is given as a control output to the input of the amplifier to actuate the robotic arm.

The position feedback is taken from the potentiometer at the end of the shaft, and the tachometer provides the velocity signal. Each of these signals are applied to the separate

channel of the A/D converter in the CHIMERA system. Due to high-frequency noise in the signal it was necessary to introduce a lowpass filter.

Several different joint angle commands were given and the tracking ability were checked in both the clockwise and counterclockwise directions. Figure 16 shows the actual joint angle response of $\theta = 46$ deg. It is to be noted that there is a vibrating motion after the joint angle has reached the terminal position. This is because of the inherent nature of the variable structure control. Once the arm reaches the terminal angle there will be a chatter which is entirely a control aspect. This chattering could be reduced by an approximate function which is given by a saturation function (3.16).

Though the sampling period could be decreased to quantize the analog signal for a better curvefitting, it has been kept long enough with a view to expand the system for more inputs and outputs in future which would require the sampling period to be decreased.

5.3 Conclusion

A control system based on the theory of variable structure control was designed and implemented using TMS320C25 processor to control joint angle of a single link robot. Implementation using DSP was of great advantage because of the speed and special instruction set which has been fully exploited in this research work. It has been observed that the closed-loop system can achieve accurate trajectory tracking.

Chapter 6

Summary

Two nonlinear control schemes were presented in this thesis to control and stabilize two link flexible robot. First we developed the model for this flexible links, taking into account all non-linearities like gravitational effect, frictional and coriolis forces coupled with flexible and rigid modes. Then the control schemes were developed such that in the closed-loop, the system asymptotically followed the representative trajcetory command while accomplishing uniform sliding motion in the variable structure control and the error states were uniformly bounded in the ultimate boundedness control scheme. The vibrating motions were suppressed by a stabilizer designed on the basis of linearized model of the robotic arm. This was switched on to give additional control for stabilizing the elastic modes when the trajectory reached the neighborhood of terminal command.

Extensive simulations were carried out and the results showed that the controllers were robust to large payload uncertainty and thus it proved these schemes to be a certain candidate for direct implementation.

An implementation of variable structure control was carried out on a single link flexible

robot, using digital signal processor. The responses were very close to the simulation results. However for stabilization of flexible modes one has to sense the the vibrating states and end point acceleration and feed them back through the stabilizer. This could be taken for future work as a continuation to this thesis, for a two link flexible robot.

Appendix A

Robot Parameters

m_1,m_2	=	5 kg	(mass of link1 and link2)
$EI1$,$EI2$	=	1000 Nm^{-2}	(stiffness of link1 and link2)
$L1, L2$	=	1 m	(length of link1 and link2)
m_j	=	1.0 kg	(joint mass at joint2)
m_p	=	4 kg	(nominal payload)
J_p	=	1 kgm^2	(inertia of payload)
$J0$	=	1.0 kgm^2	(inertia of mass at joint1)
$J01$	=	0.8 kgm^2	(inertia of mass at joint2)

Bibliography

1. Maizza-Neto, O.,"Modal analysis and control of flexible manipulator arms", Ph.D Thesis, Dept.of Mechanical Engineering,M.I.T., Cambridge, 1973.

2. Book, W. J.,Maizza-Neto, O. M., and Whitney, D. E.,"Feedback control of two-beam, two-joint systems with distributed flexibility,"
J.Dynamic Systems Measurements and control., vol 94,4,pp.424-431,
Dec.1975.

3. Book, W. J., and Majette, M.,"Control strategy for flexible robot mechanism arm via combined state space frequency domain techniques ", Journal of dynamic systems Measurements and Control., vol 105, pp 254-274, Dec.1983.

4. Chalhoub, N.G., and Ulsoy, A. G.,"Control of a Flexible Robot Arm: Experimental and theoritical result", J.Dynamic Systems Measurements and Control, vol 109, pp 299-309, Dec 1987.

5. Usora, P. B., Nadira, R., and Mahil, S. S.,"Control of lightweight flexible manipulators : A feasibility study", in Proceedings of the 1984 American Control Conference., pp.

1209-1216, 1984.

6. Balas, M.J," Feedback control of flexible systems", IEEE Transaction Automatic Control. AC-23(4), 673-679.

7. Fukuda, T."Flexibility control of elastic robotic arms", Journal of Robotic Systems 1985, 73-88.

8. Sakawa, Y, Matsuno, F., and Fukushima," Modeling and feed- back control of a flexible arm", Journal of Robotics Systems, 1985,453-472.

9. Cannon, Jr. R.H.,and Schmitz, E,"Initial experiments on the end-point control of a flexible one-link robot", Int. J.Robotics Res.1984, 62-75.

10. Nemir, D. C., A.J.Koivo and Kashyap, R. L.,"Pseudolinks and the self-tuning control of a nonrigid link mechanism", IEEE Transactions on Systems, Man and Cybernetics, vol.18, pp.40-48, Jan/Feb 1988.

11. Hastings, G.G., and Book, W.J.," Experiments in optimal control of a flexible arm", Proc.1985 American control Conference, pp 728-729. New York.

12. Yerkovich. Stephen,"On Controller Tuning for a Flexible-Link Manipulator with varying Payload", Journal of Robotic Systems, June 1989.

13. Singh, S. N., and Schy, A. A.,"Elastic robot control:nonlinear inversion and linear stabilization", IEEE Transactions on Aerospace and electronic Systems, vol 22, pp

340-348, Sept.1986.

14. Singh, S. N., and Schy, A. A., "Control of Elastic Robotic Systems by Nonlinear Inversion and Modal damping", Journal of Dynamic System, Measurement and Control, vol.108, Sept. 1986, pp 180-189.

15. Das, A. and Singh, S. N.,"Dual mode control of an elastic robotic arm: nonlinear inversion and stabilization by pole assignment", American Control Conference, June 1989.

16. Khorasani, K., and Spong,M.W," Invariant manifolds and their application to robot manipulators with flexible joints", Proc. 1985 IEEE International Conference on Robotics and Automation, pp 978-983. New York : IEEE

17. Marino, R., and Nicosia,S,"On the feedback control of industrial robots with elastic joints: A singular perturbation approach", Rep.84.01. Roma, Italy: Seconda Universita di Roma, Dipartimento di Ingegneria Elettronica, 1984.

18. Bruno Siciliano, Wayne J.Book 1988, "A Singular Perturbation approach to control of Lightweight Flexible Manipulators", The International Journal of Robotics research, vol.7, No.4 1988, pp 79-88.

19. Singh, S.N.,"Control and stabilization of a nonlinear uncertain elastic arm," IEEE Transaction on Aerospace and Elastic Systems, pp 148-155, March 1988.

20. Nathan, P.J. and S. N. Singh, "Variable Structure control of a robotic arm with flexible links", IEEE International Conference on Robotics and Automation, May 1989, pp 882-887.

21. Utkin, V.I.,*Sliding Modes and their application in variable structure system*, 1978 MIR Publishers, Moscow.

22. Itkis, U., *Control Systems of Variable Structure, John Wiley and Sons*, New York, 1976.

23. Balestrino, A., DeMaria, G., Zinobes,A.S.,"Nonlinear Adaptive Model following Control", Automatica, vol. 21, No.5, 1984, p559-568

24. Nicosia, S.and Tomei, P.,"Model Reference Adaptive control Algorithms for Industrial Robots", Automatica, 1984, p.635-644

25. Slotine.J.J. and Sastry.S.S.,"Tracking Control of Nonlinear Systems using Sliding Surfaces with application to Robot Manipulators", International Journal of Control, vol.38, No.2, 1981, p.465-492.

26. Paden.B.E. and Sastry.S.S.,"Calculus for computing Fillippov's Differential Inclusion with application to the Variable Structure control of Robot Manipulator", IEEE Transactions on Systems and circuits,

vol.34, Jan.1987, pp 73-82.

27. Young, K. D.,"Controller Design for a manipulator using Theory of Variable Structure systems", IEEE transactions on Systems, man and Cybernetics, vol.SMC-8, No.2, February 1978.

28. Singh, S. N and Zakharia, Y. N.,"Variable Structure Control of a Puma arm in presence of uncertainty", Journal of Robotic Systems, April 1989 (to appear).

29. Ambrosino, G., Celentano, G., and Garofalo, F. (1985) "Robust tracking control of nonlinear plants", IEEE Transaction on Automatic Control Vol. AC-30, (1985), pp 275-279.

30. Ambrosino, G., Celentano, G., and Garofalo, F. (1985) "Adaptive tracking control of industrial robots", IEEE Journal of Dynamic Systems. Measurement and control, Vol. 110, (1988), pp 215-220

31. Singh, S.N., "Decoupled Ultimate Boundedness Control of Systems and Large Aircraft Maneuver", IEEE Transactions on Aerospace and Electronic systems Vol. 25, No.5., September 1989.

32. Leitmann, G.,"On the efficacy of nonlinear control in uncertain linear systems", Journal of Dynamic Systems, Measurement and Control, Vol. 102, 1981, pp 95-102.

33. Robert van der Kurk and J. Scannell, "Motion Controller employs DSP technology", *PCIM*, September 1988.

34. C.L. Philips and H.T. Nagle, Jr., *Digital Control System Analysis and Design*, Printice Hall Inc., 1984.

35. Texas Instruments Ltd., *Digital Signal Processing application with TMS320 family*, 1987.

36. Texas Instruments Ltd., *Second-Generation TMS320 User's Guide*, 1987.

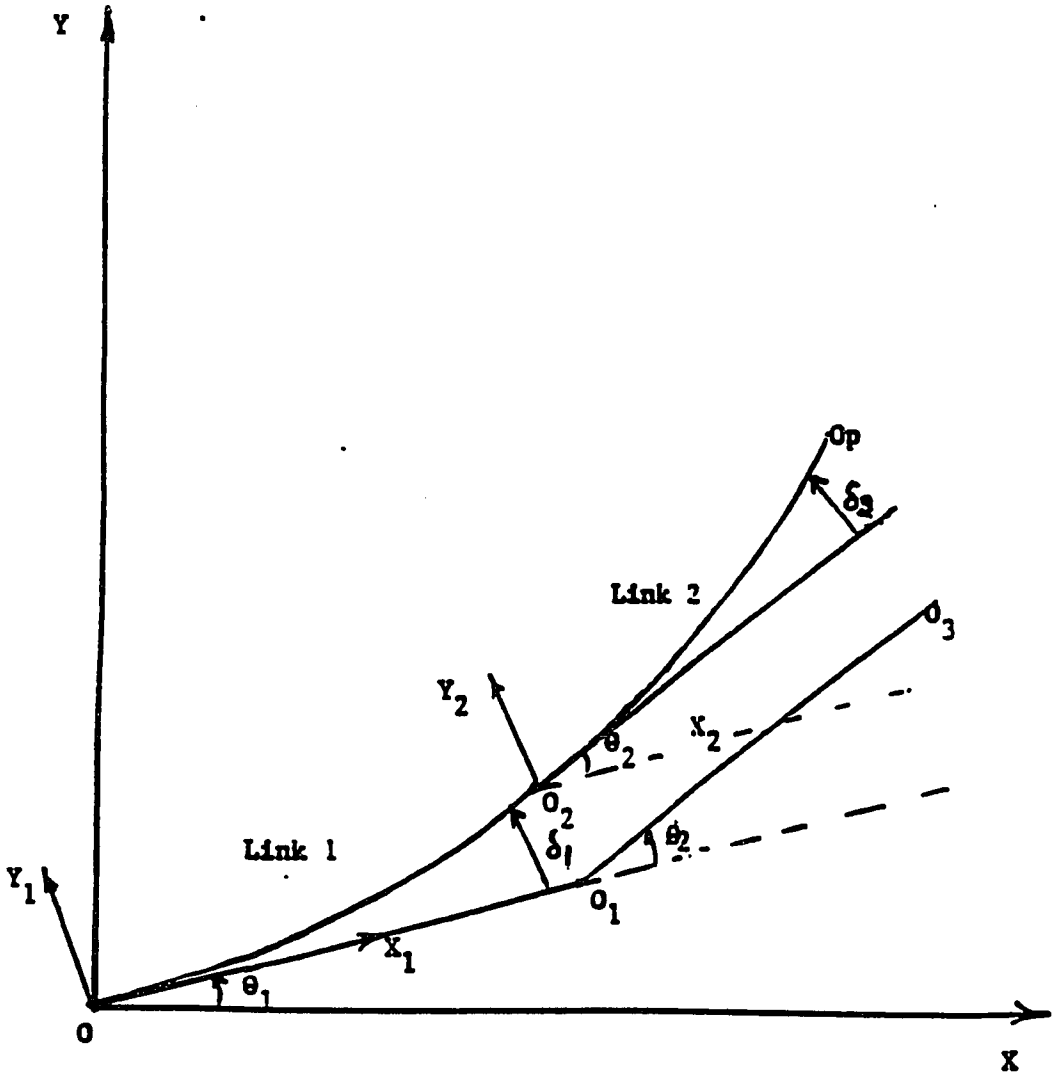

Elastic Robot with two flexible links

Figure 1

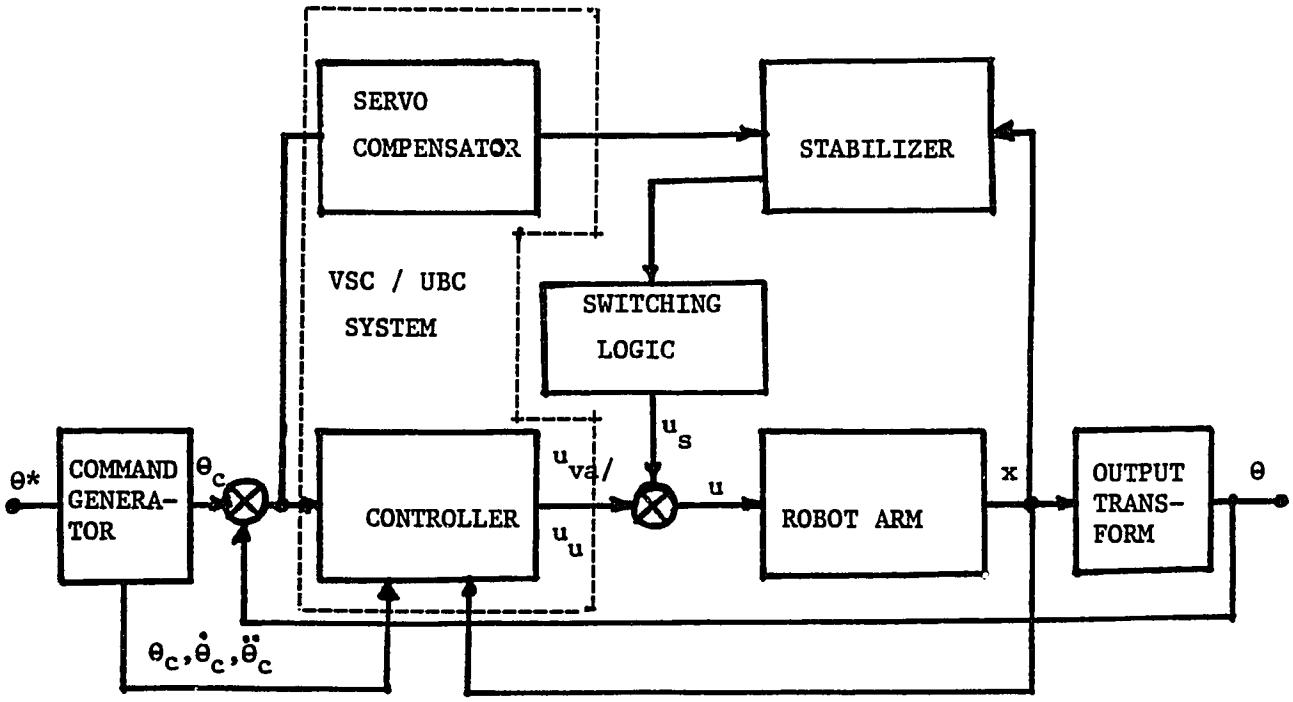

VSC/UBC System

Figure 2

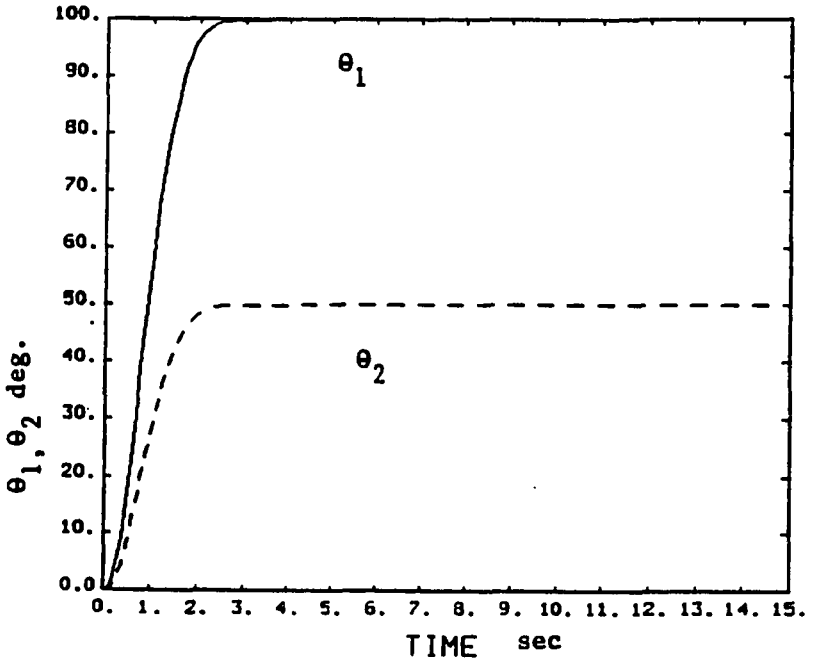

Figure 3(a)

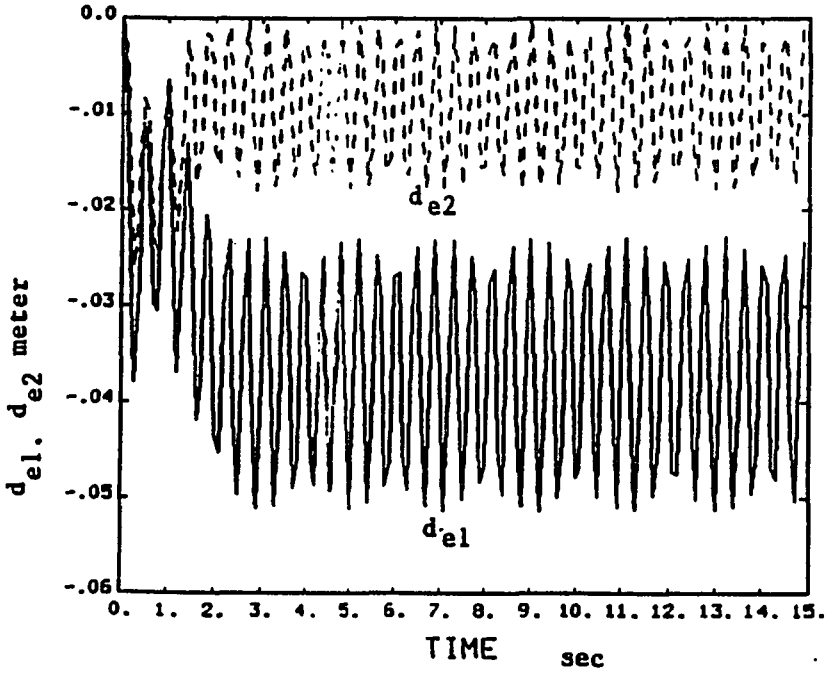

Figure 3(b)

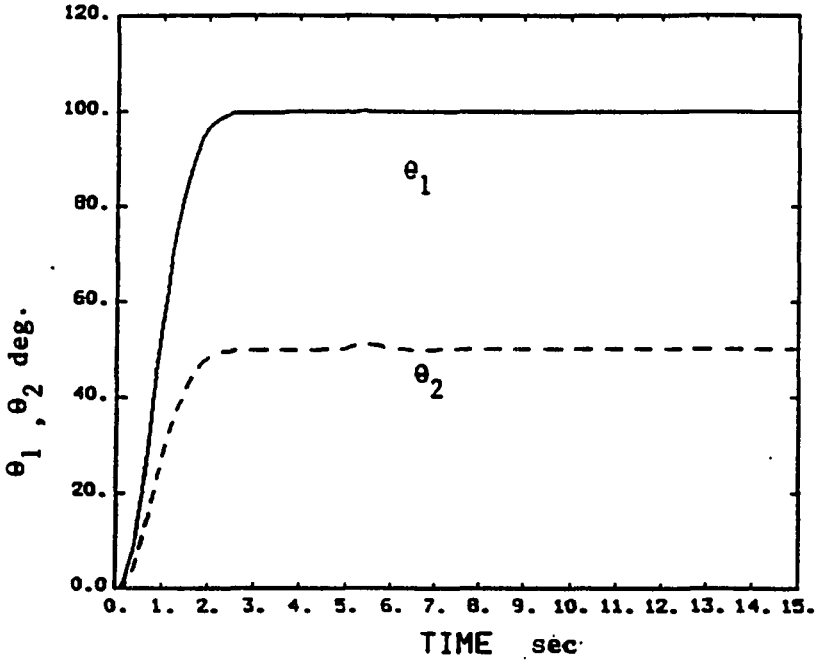

Figure 4(a)

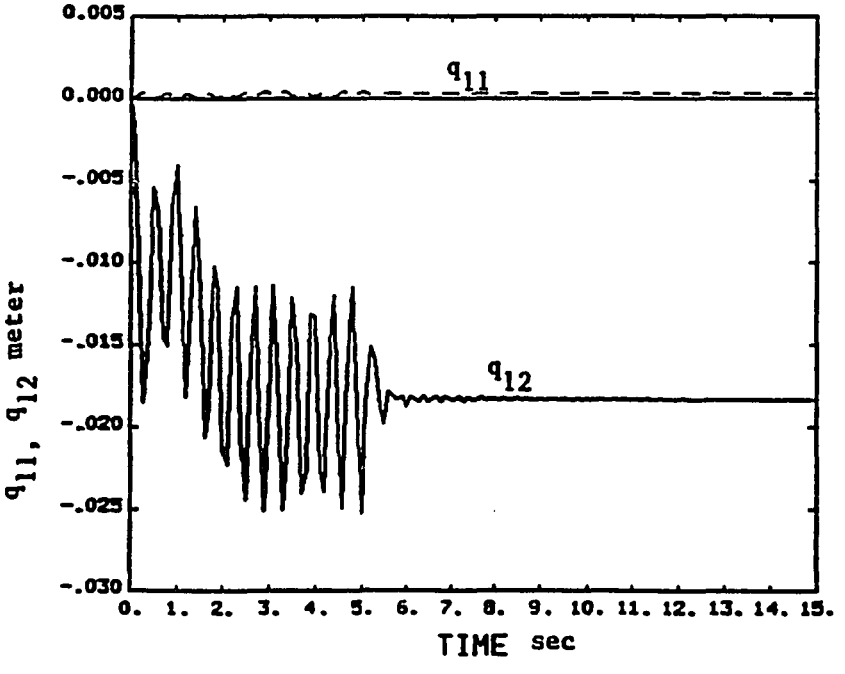

Figure 4(b)

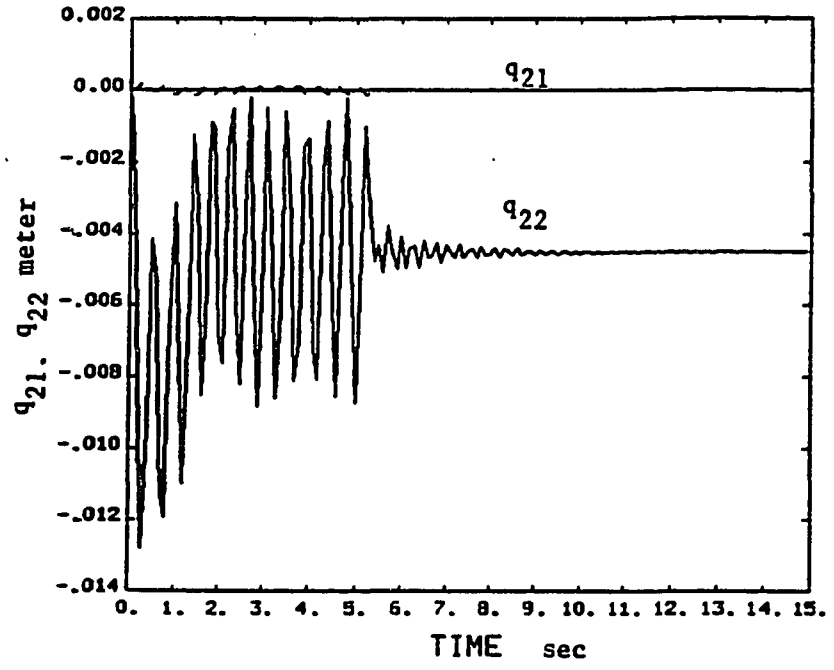

Figure 4(c)

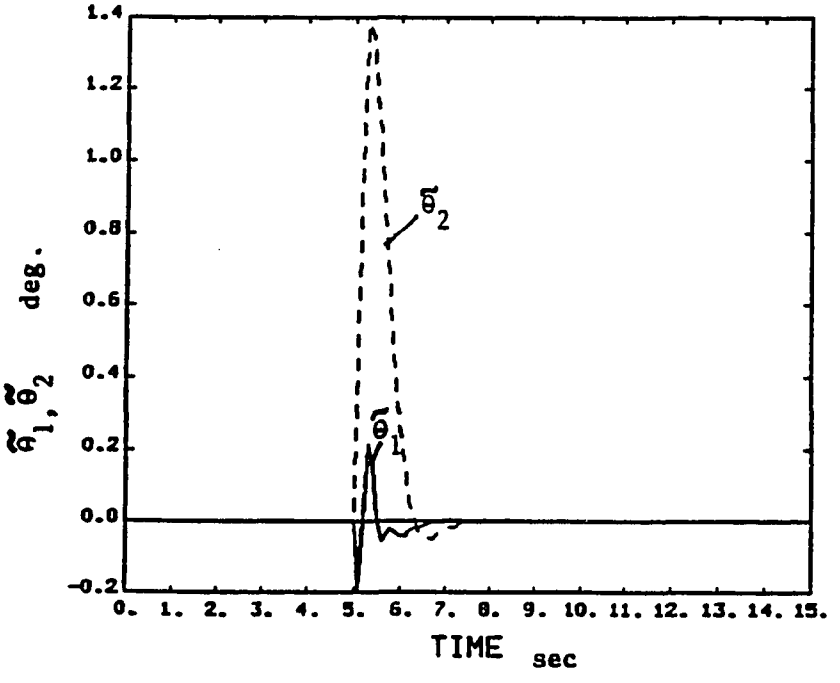

Figure 4(d)

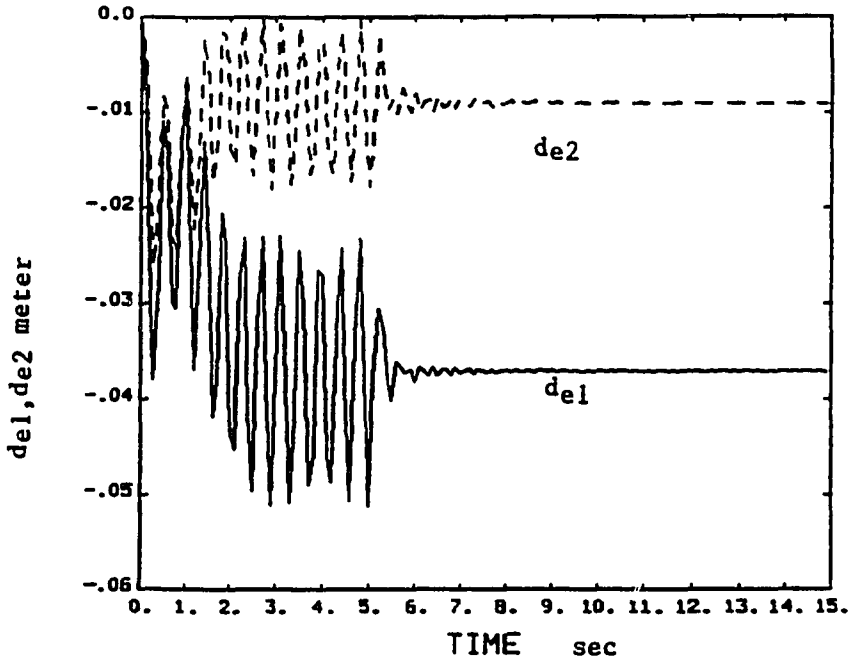

Figure 4(e)

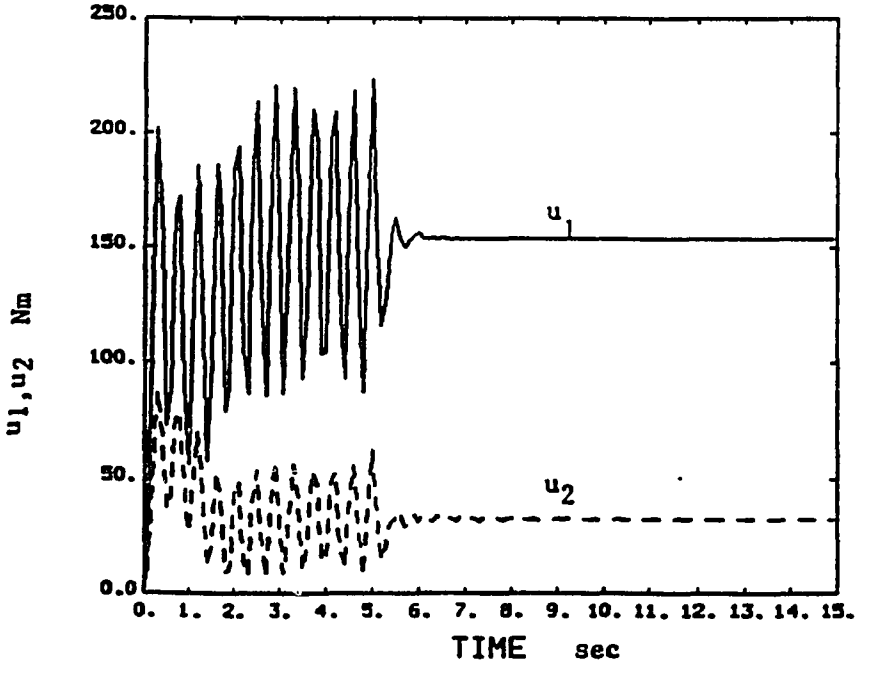

Figure 4(f)

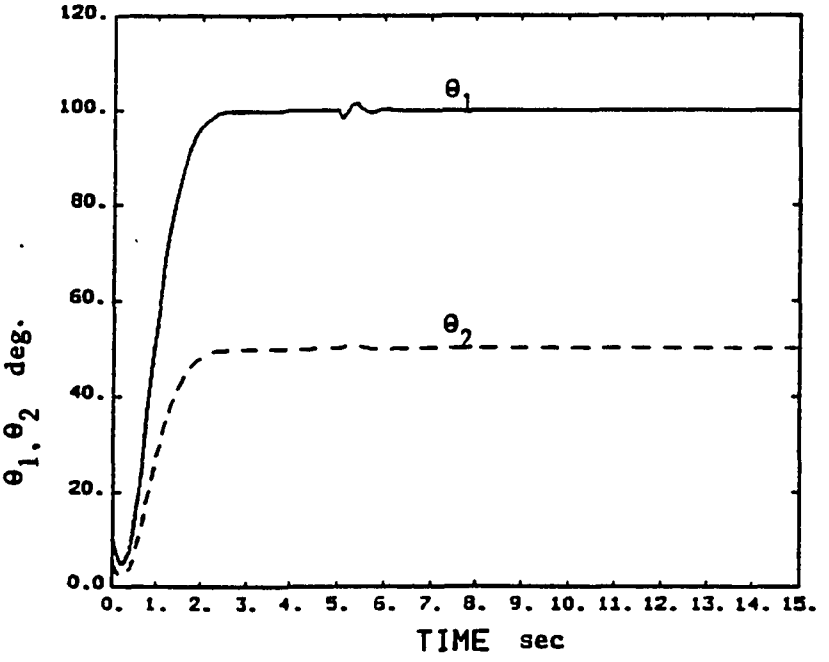

Figure 5(a)

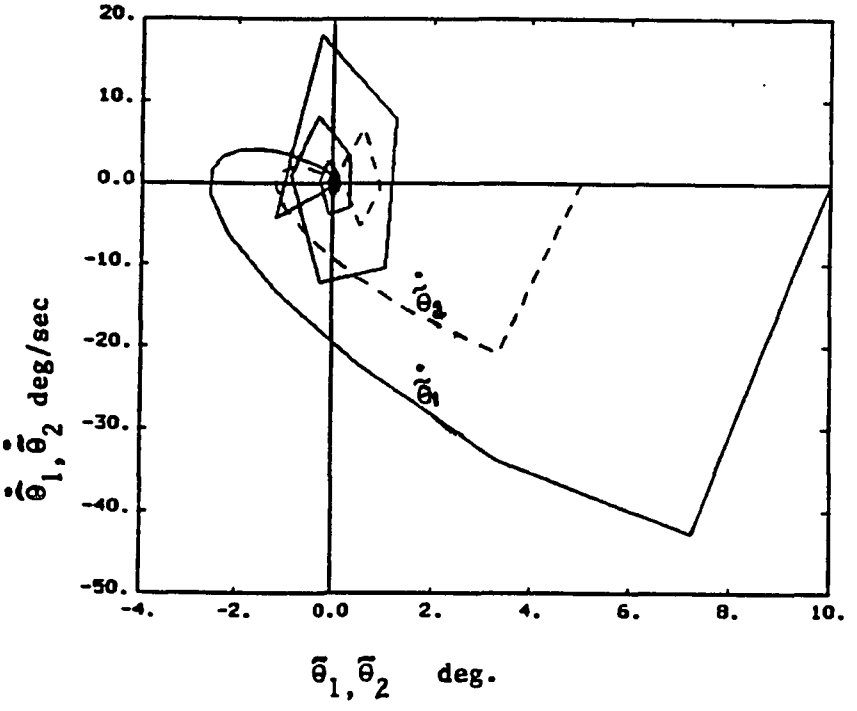

Figure 5(b)

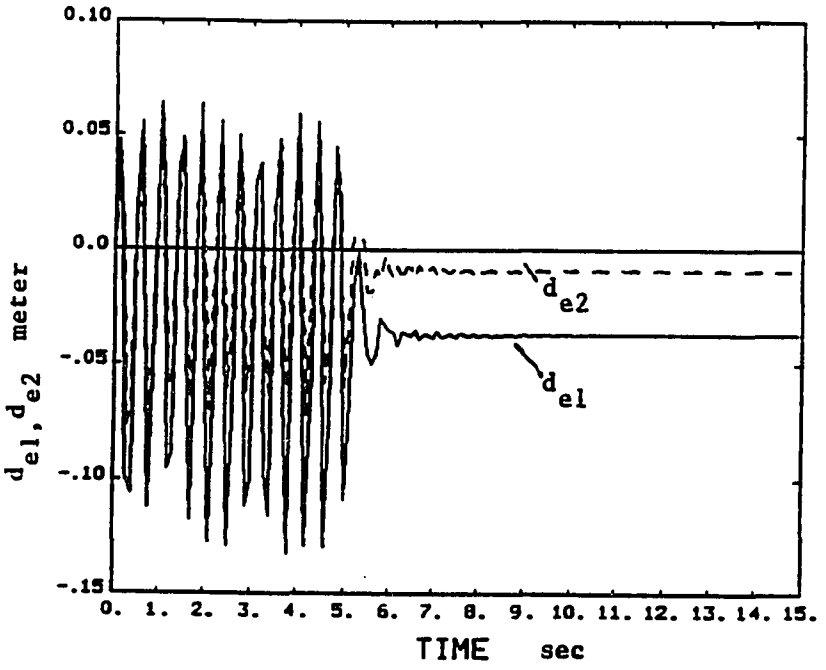

Figure 5(c)

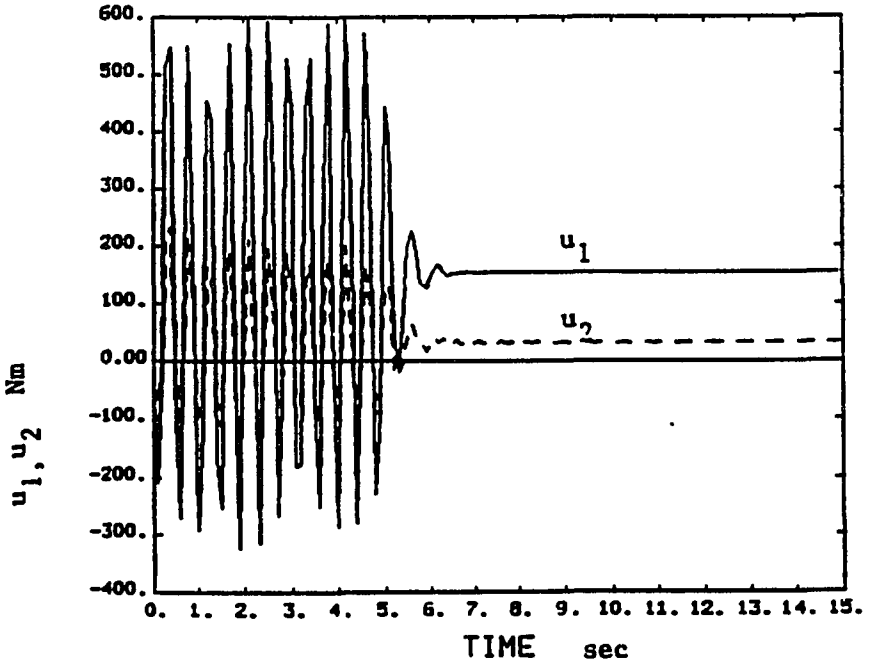

Figure 5(d)

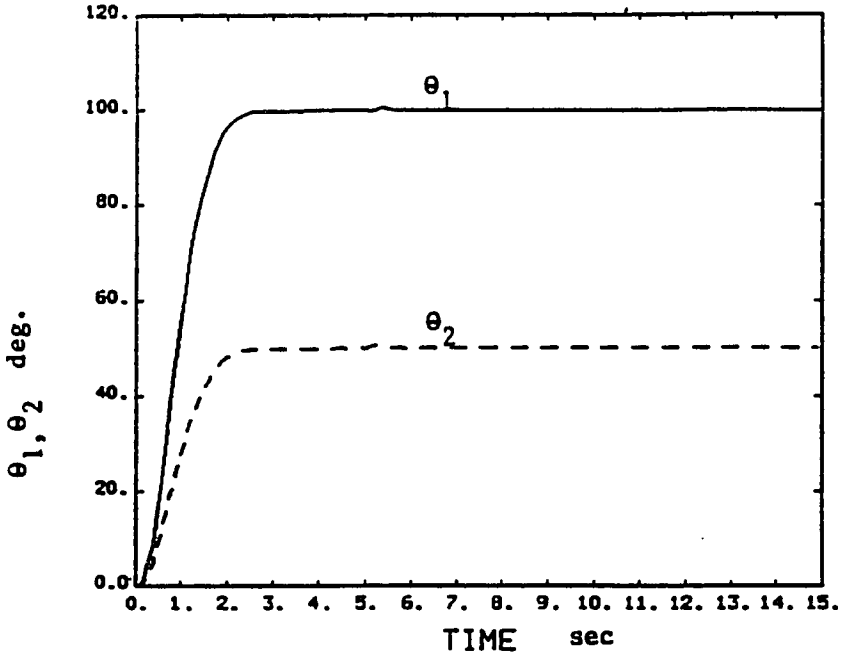

Figure 6(a)

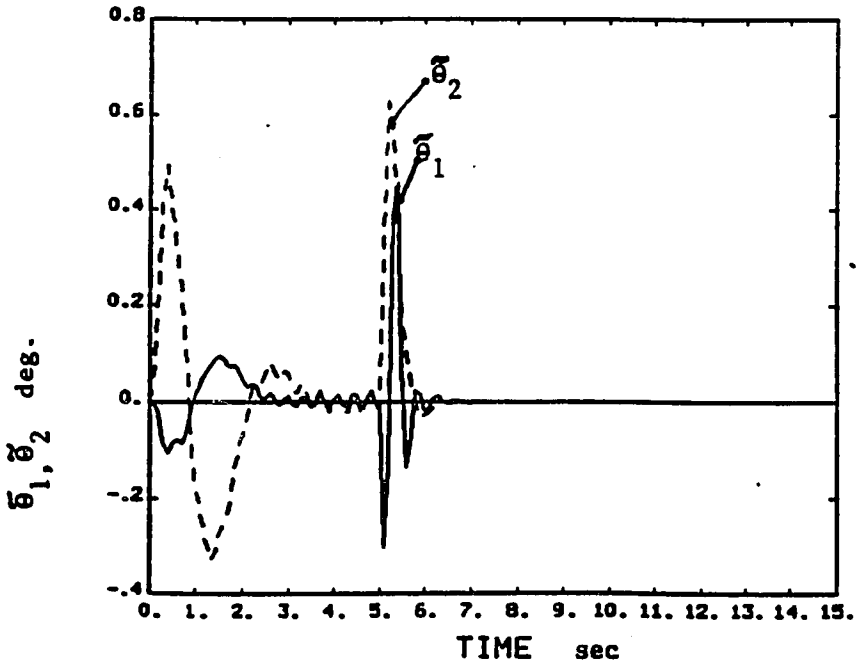

Figure 6(b)

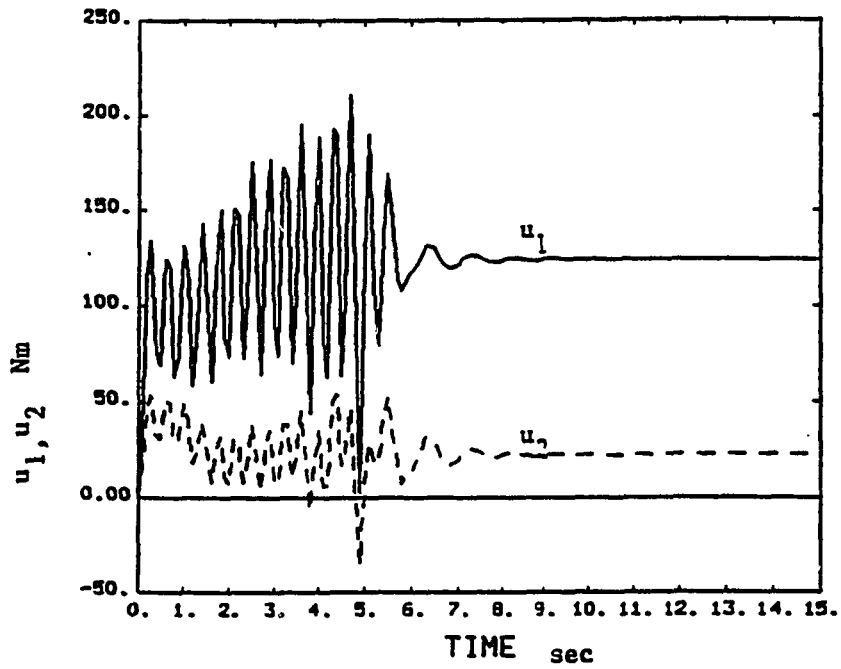

Figure 6(c)

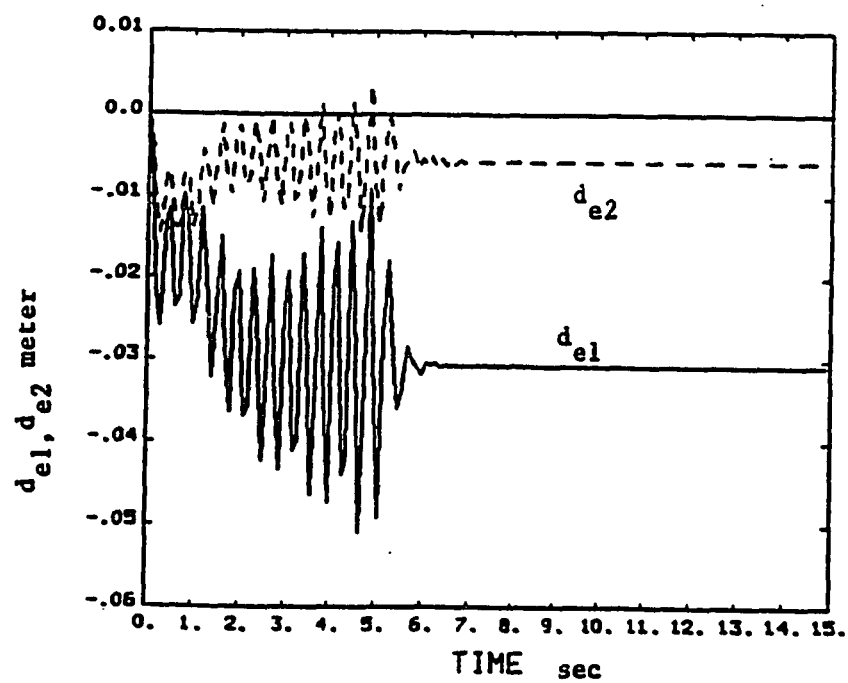

Figure 6(d)

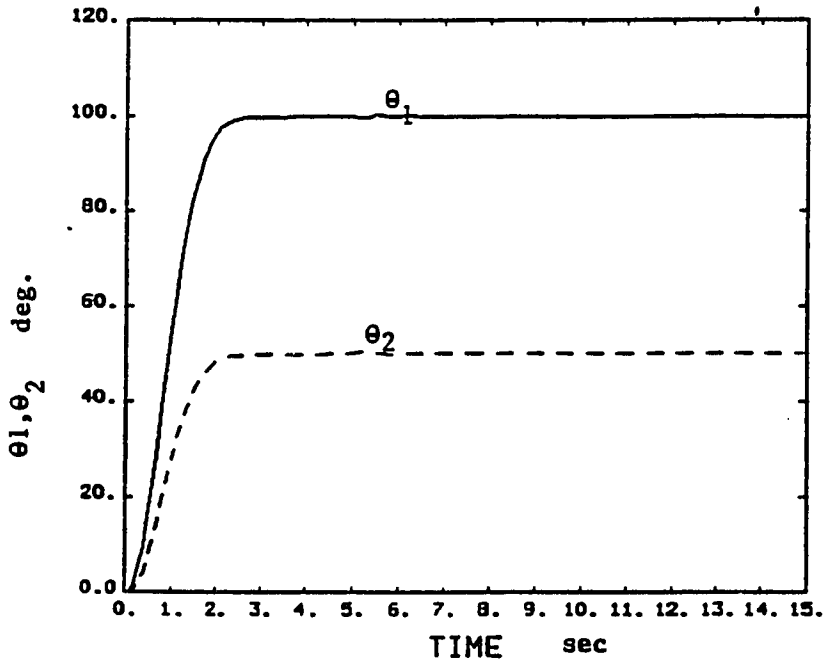
120.
100.
80.
60.
40.
20.
0.0
θ1
θ2
θ1,θ2 deg.
0. 1. 2. 3. 4. 5. 6. 7. 8. 9. 10. 11. 12. 13. 14. 15.
TIME sec

Figure 7(a)

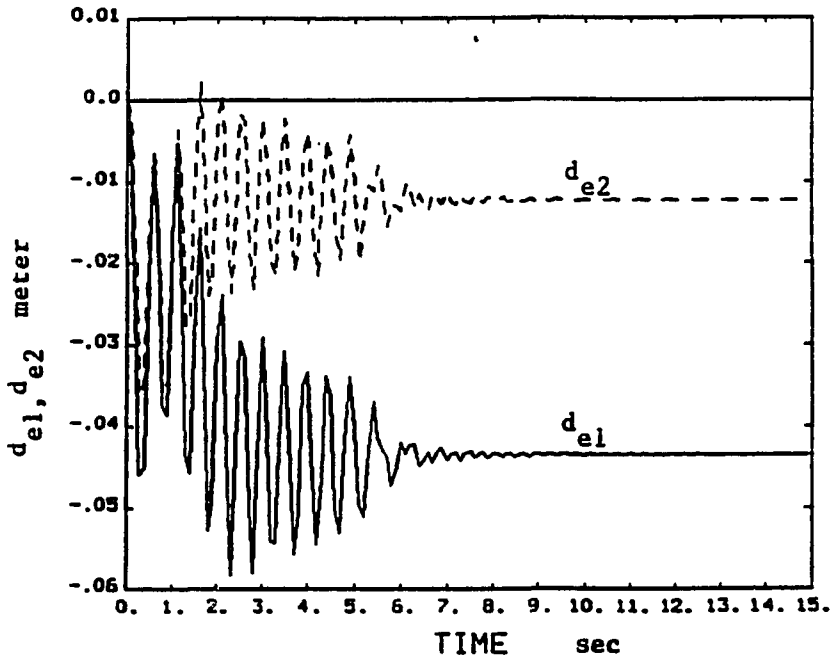

Figure 7(b)

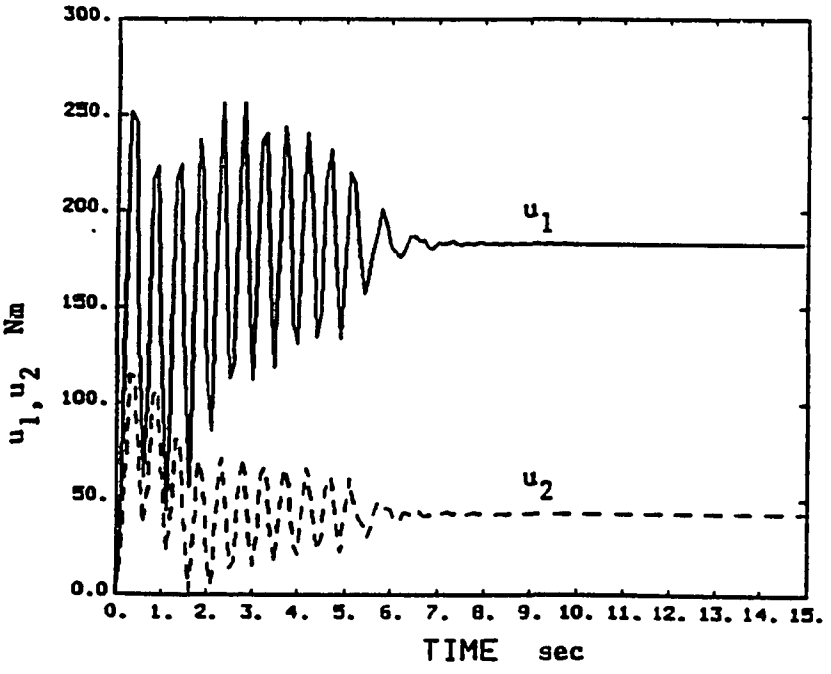

Figure 7(c)

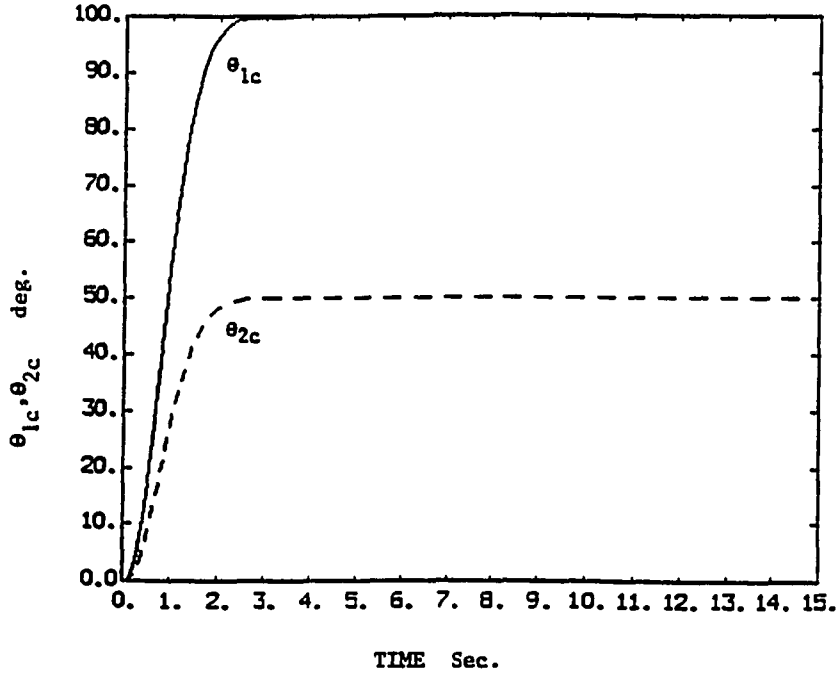

Figure 8(a)

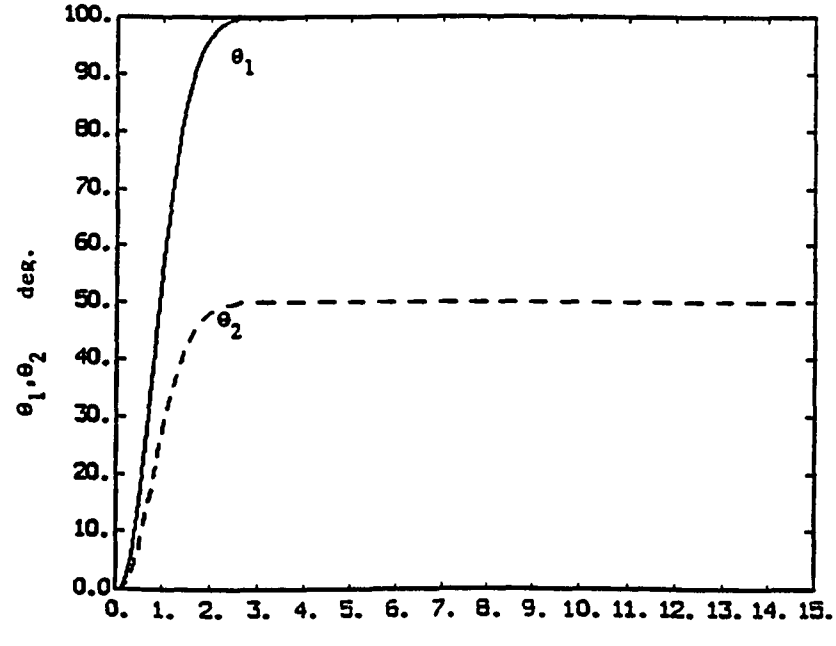

Figure 8(b)

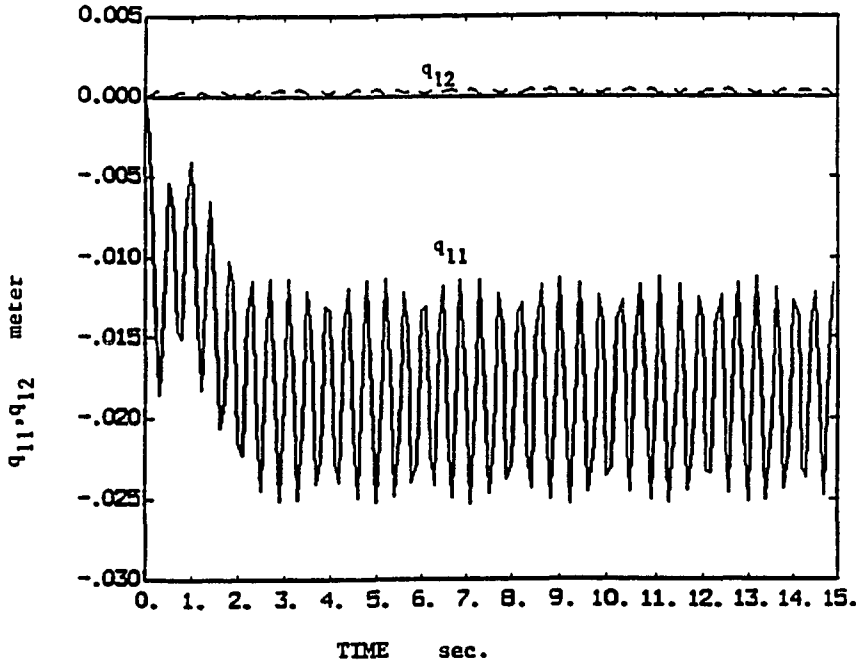

Figure 8(c)

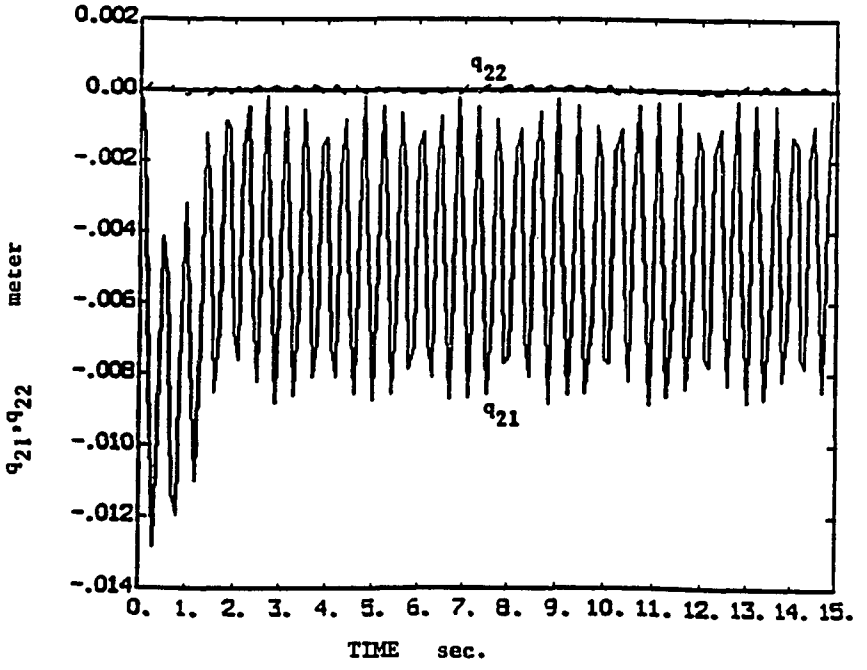

Figure 8(d)

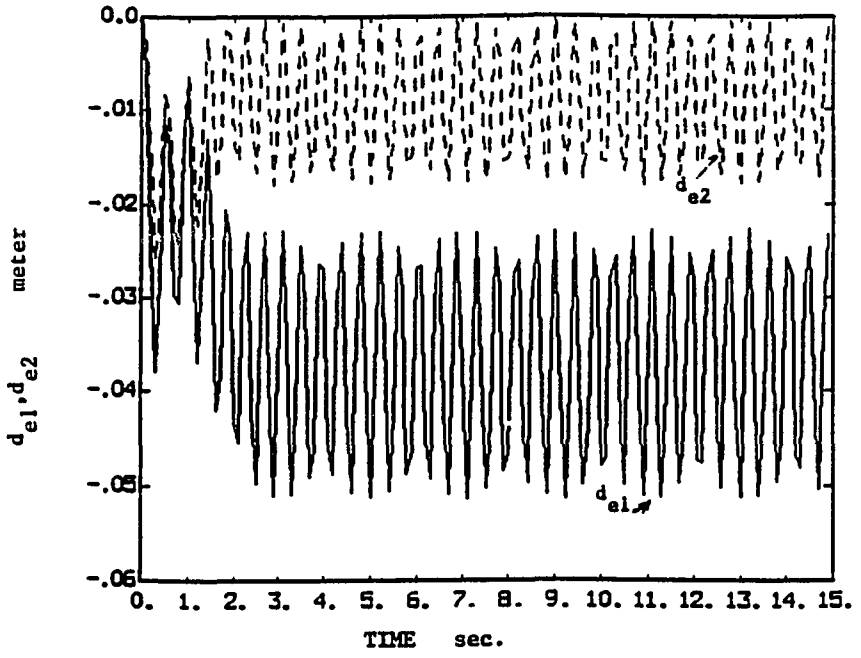

Figure 8(e)

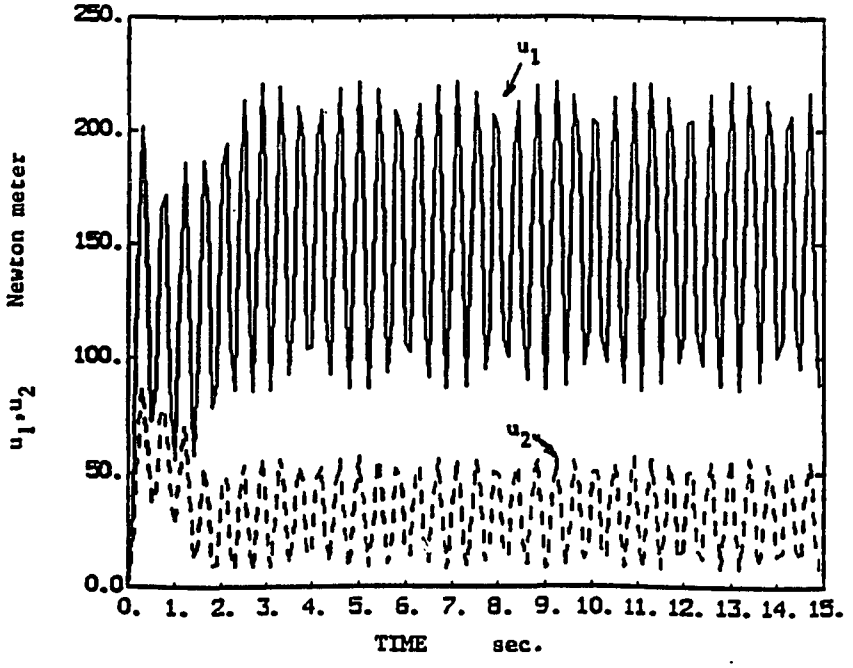

Figure 8(f)

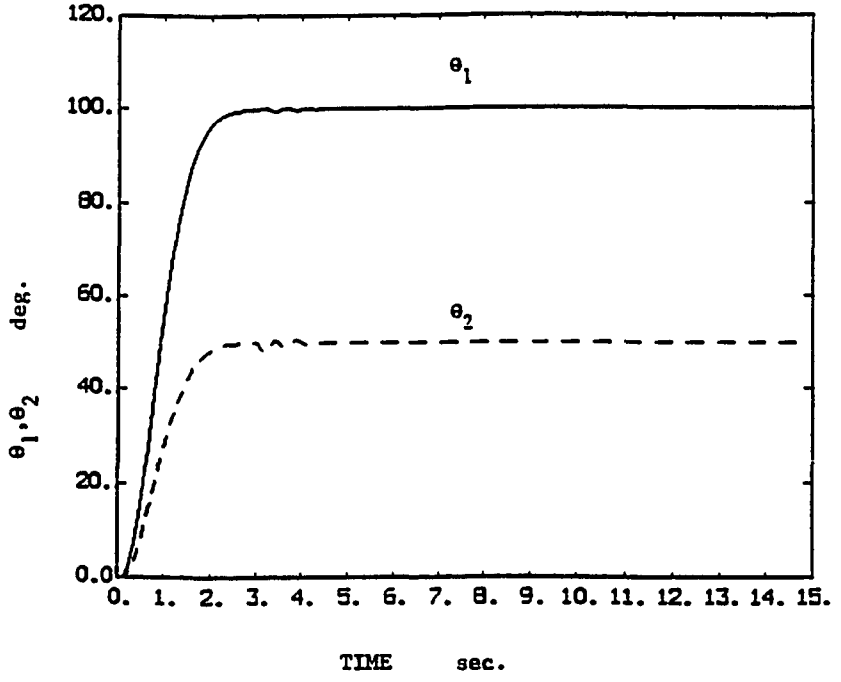

Figure 9(a)

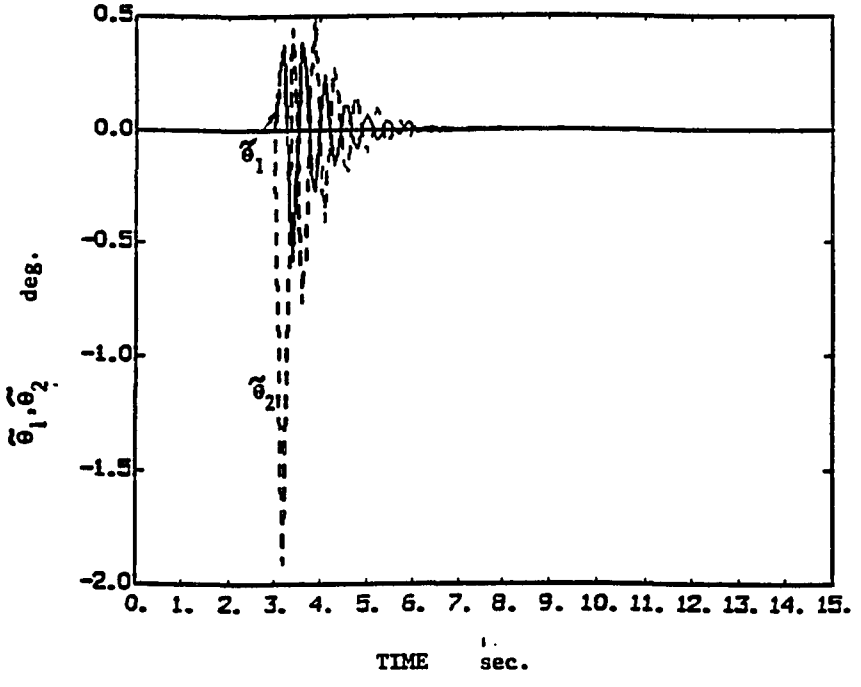

Figure 9(b)

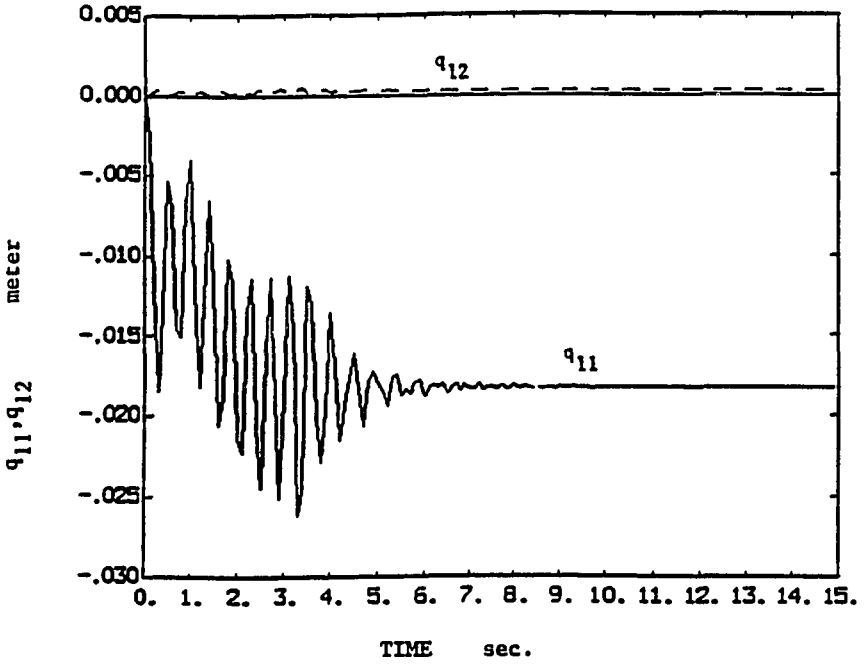

Figure 9(c)

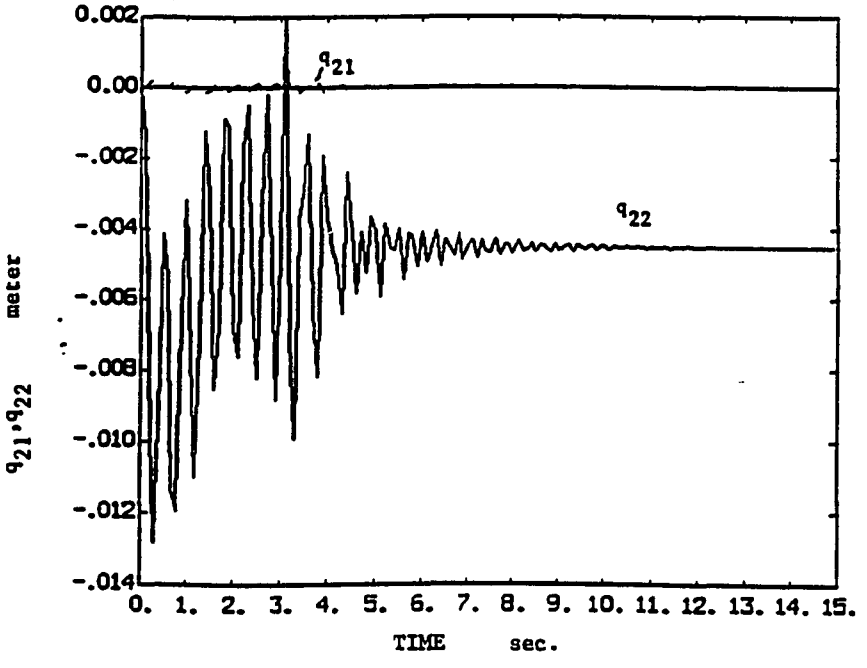

Figure 9(d)

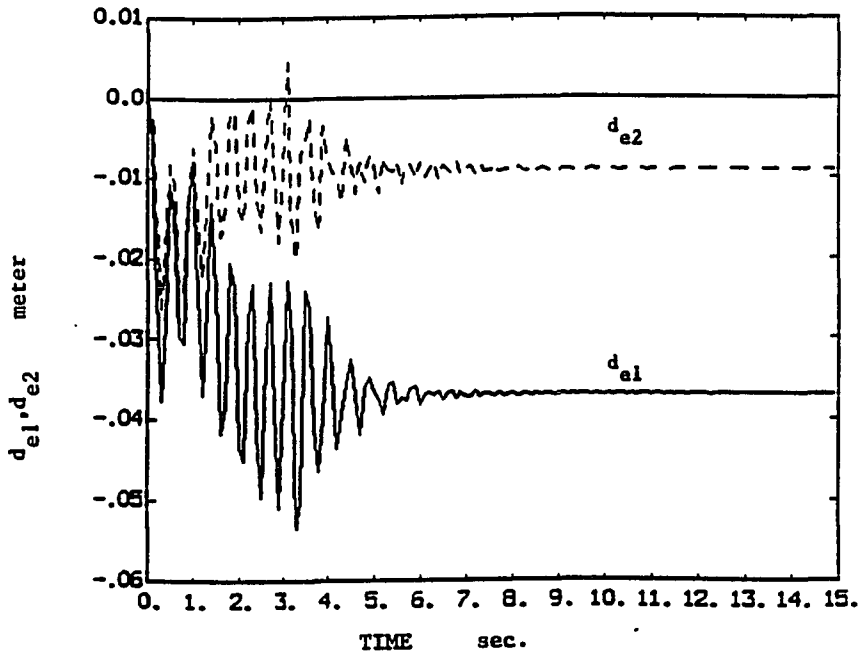

Figure 9(e)

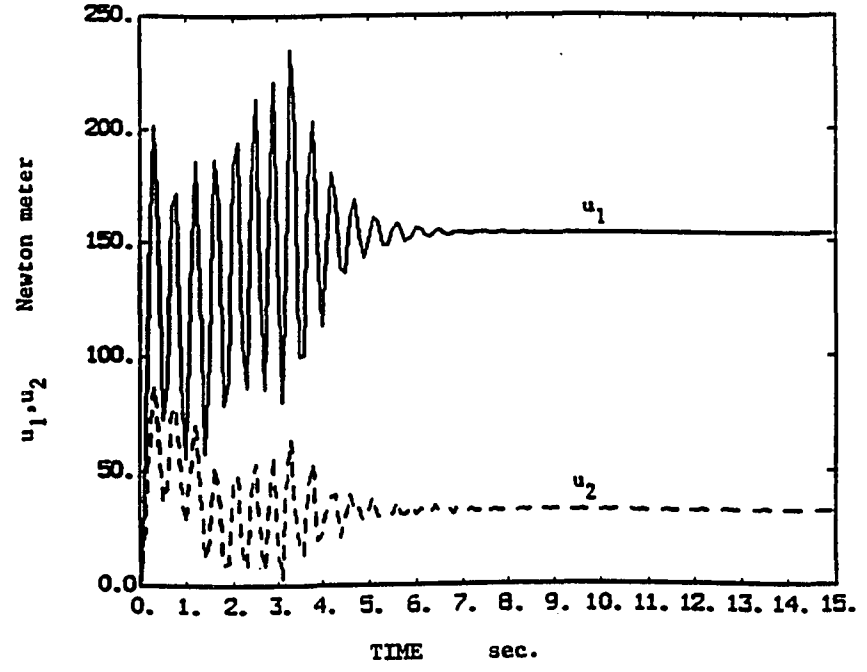

Figure 9(f)

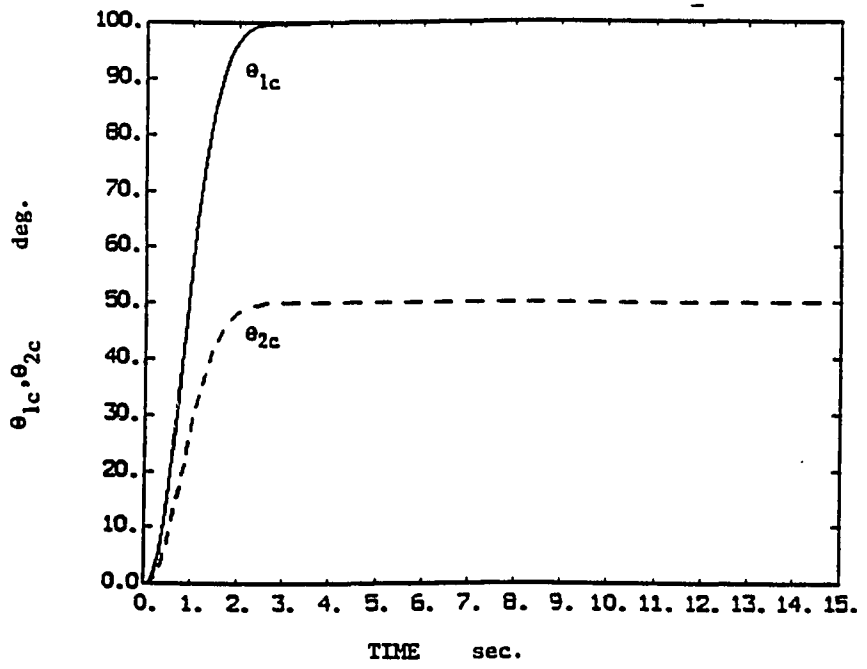

Figure 10(a)

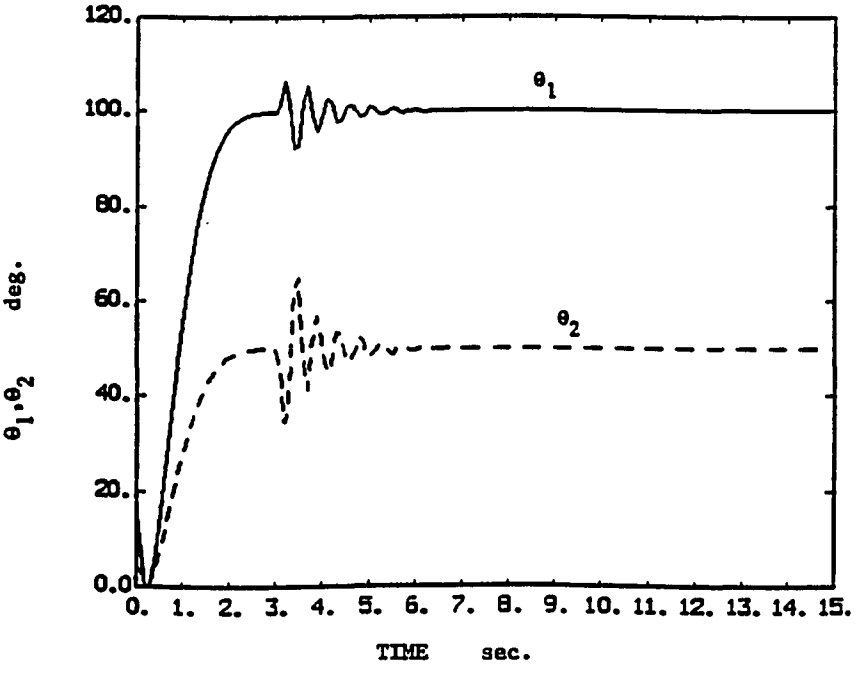

Figure 10(b)

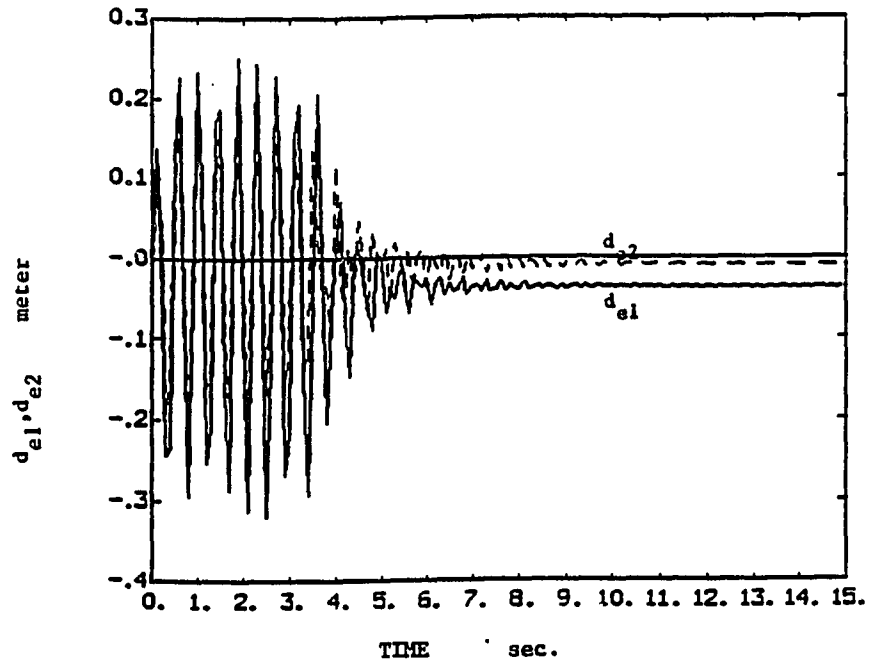

Figure 10(c)

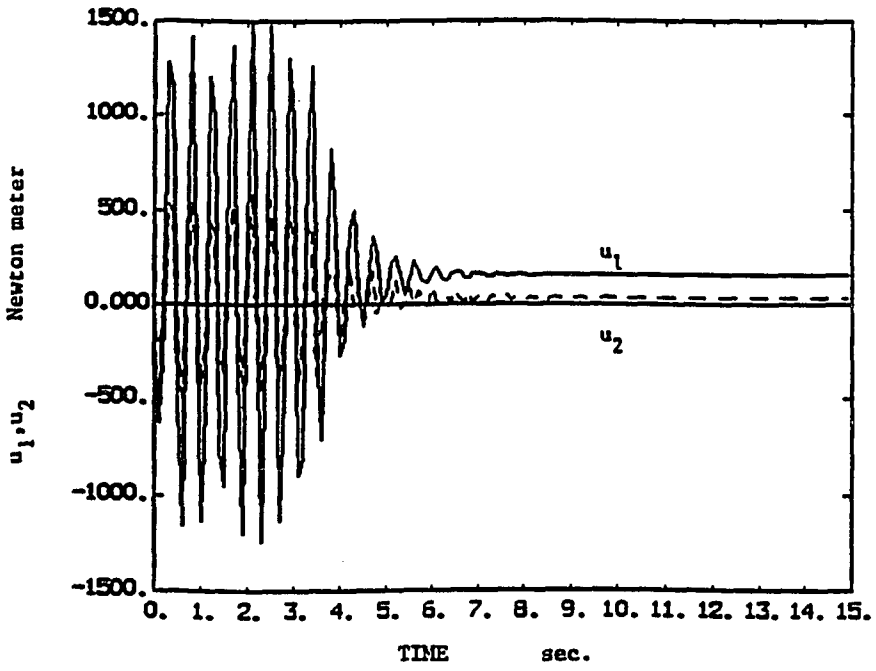

Figure 10(d)

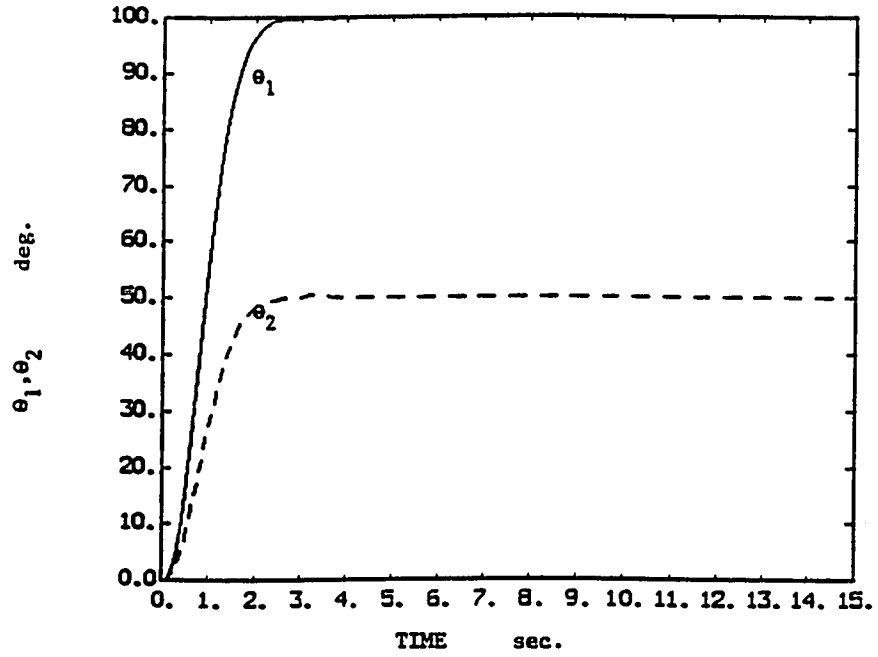

Figure 11(a)

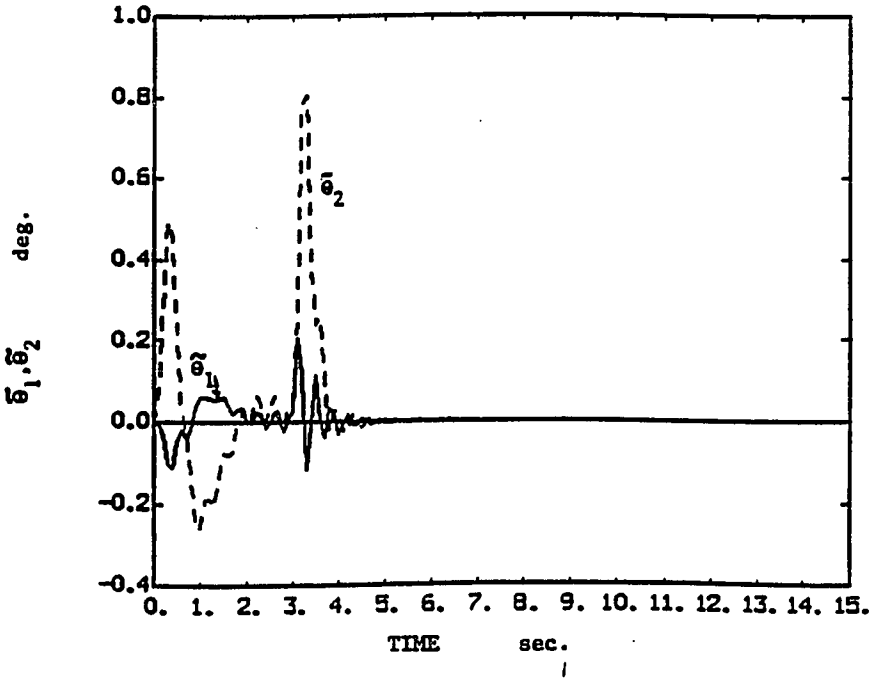

Figure 11(b)

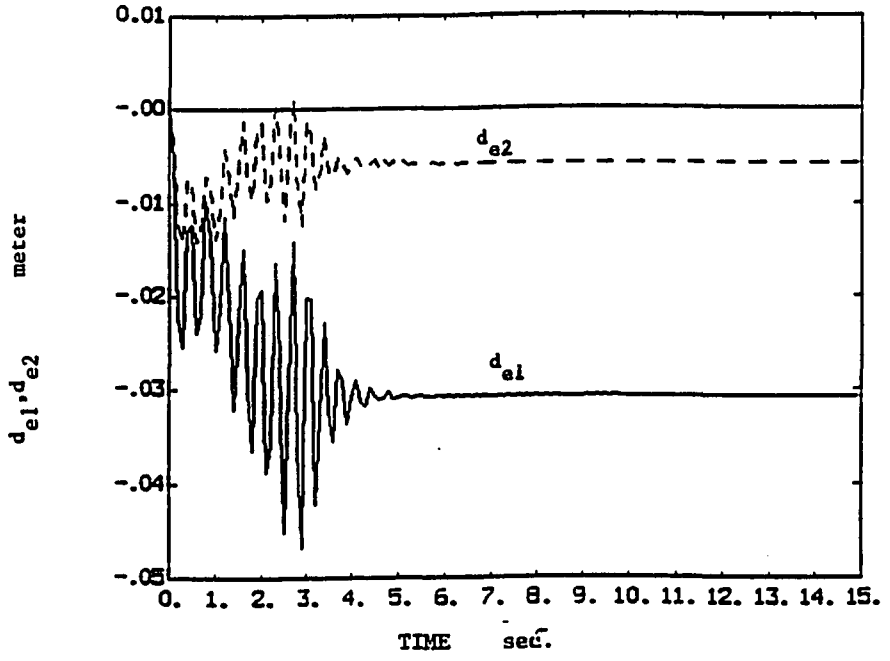

Figure 11(c)

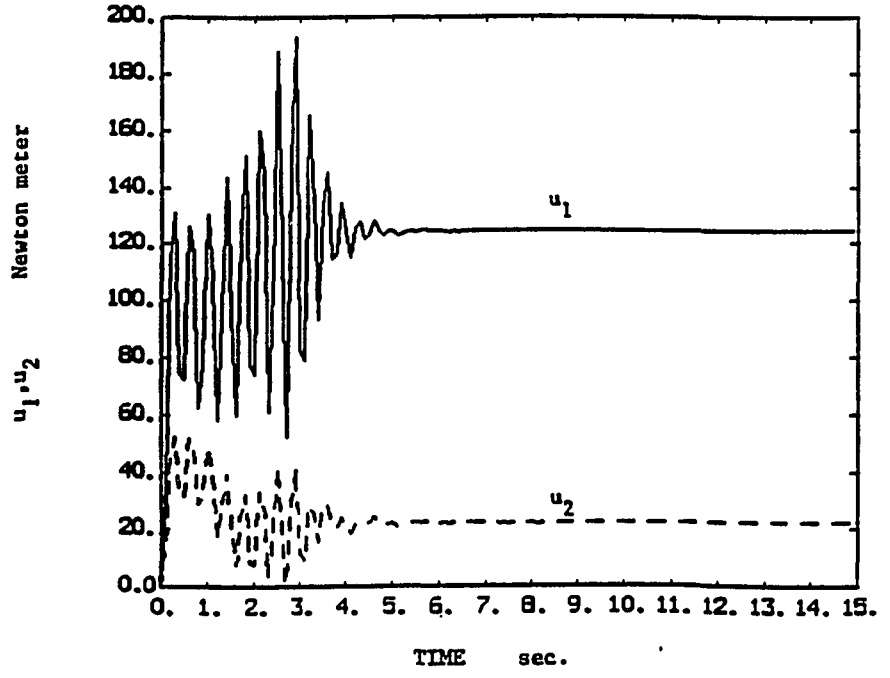

Figure 11(d)

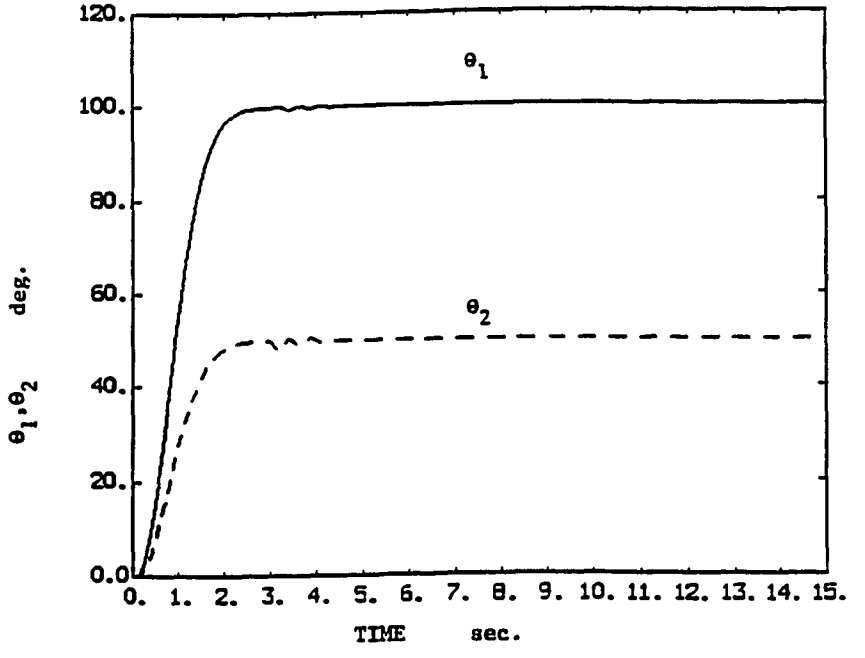

Figure 12(a)

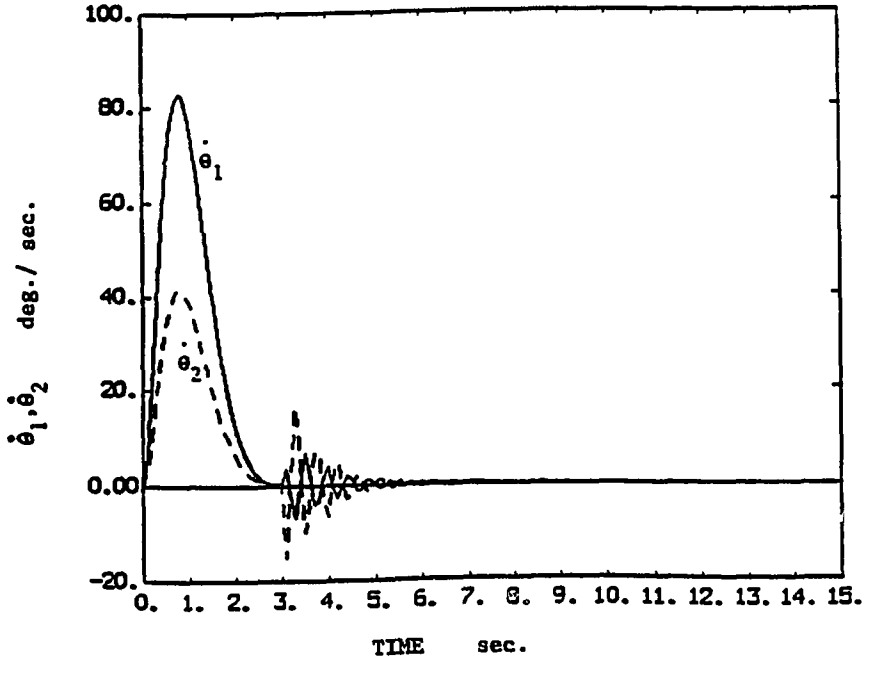

Figure 12(b)

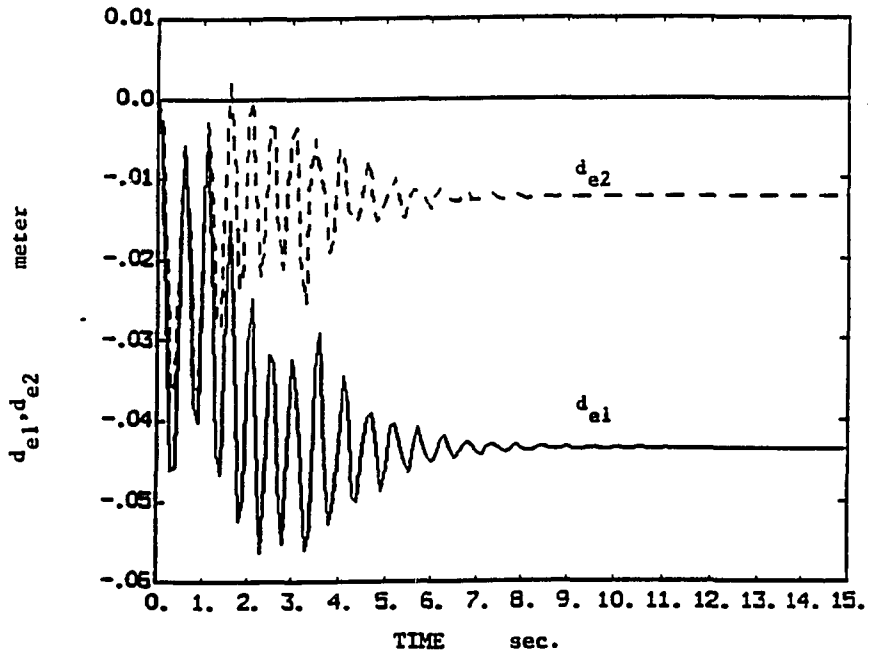

Figure 12(c)

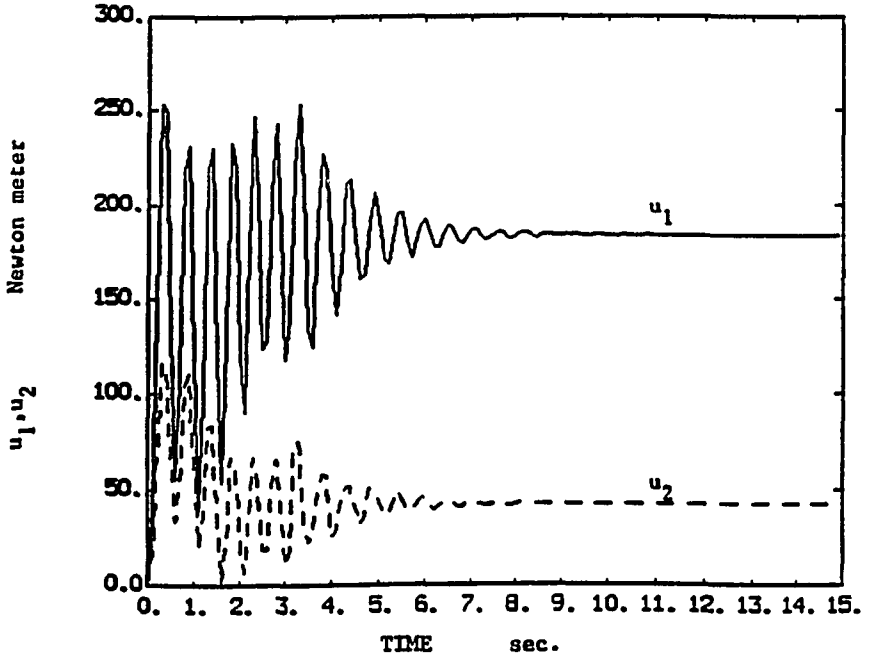

Figure 12(d)

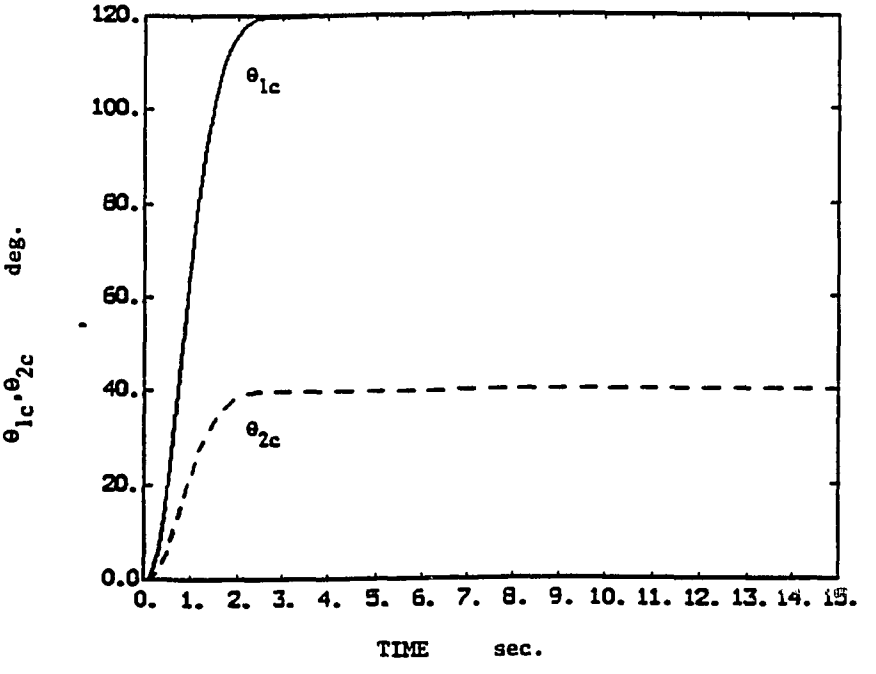

Figure 13(a)

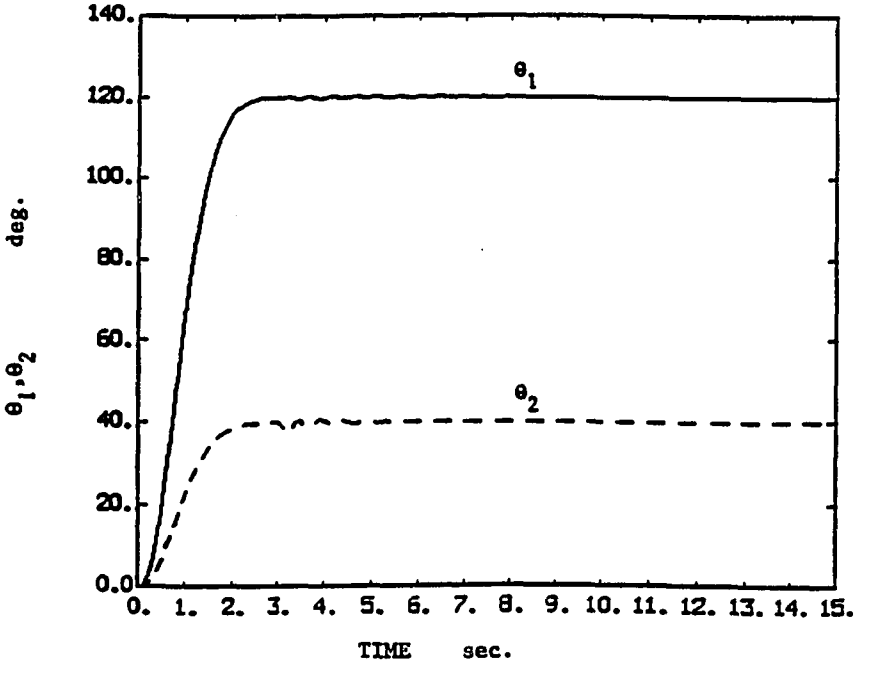

Figure 13(b)

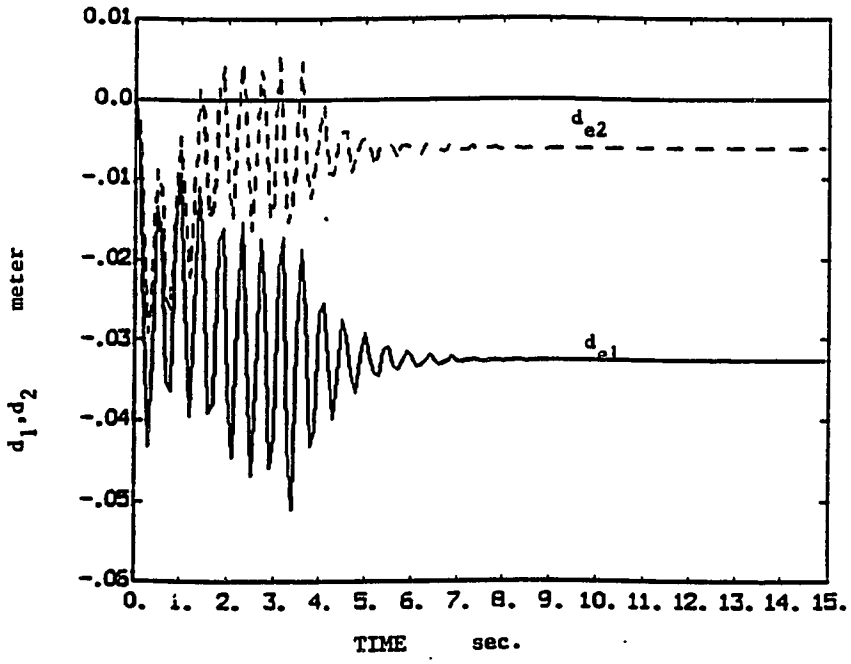

Figure 13(c)

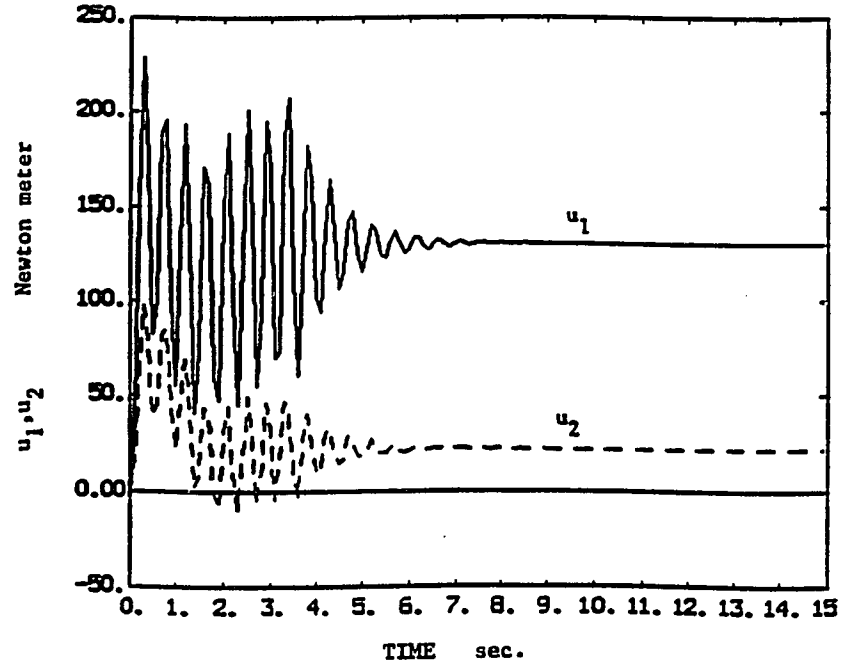

Figure 13(d)

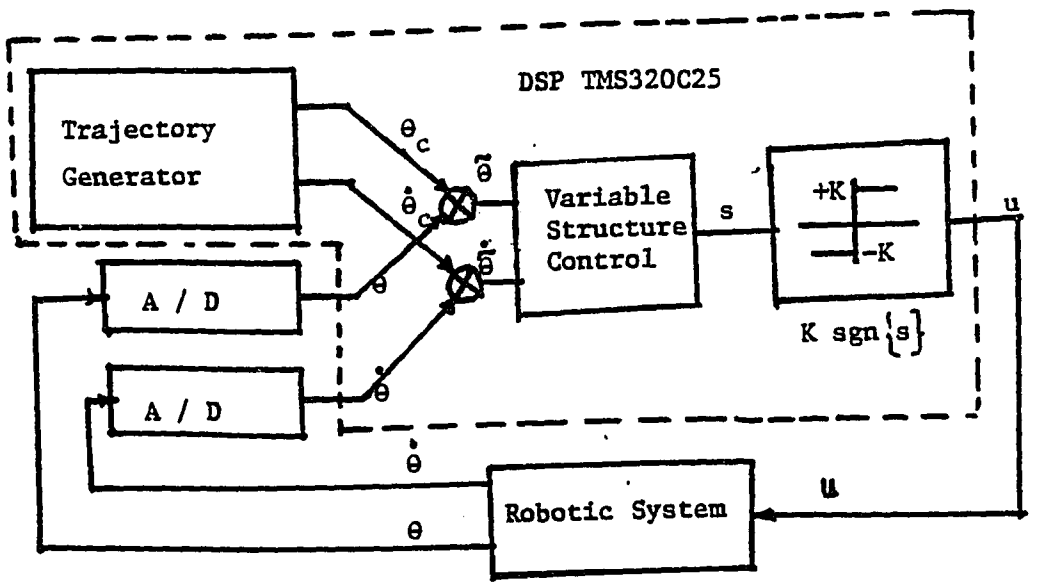

Digital Control System

Figure 14

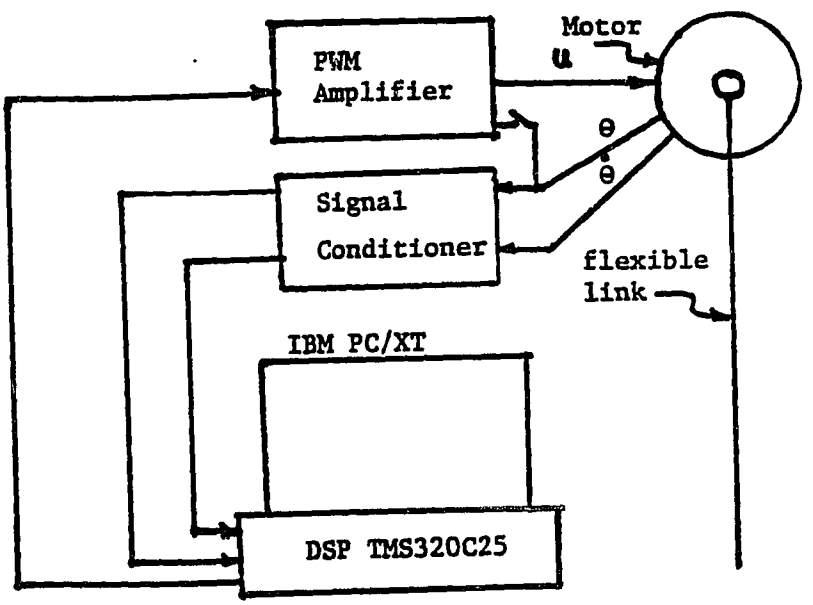

Experimental Setup

Figure 15

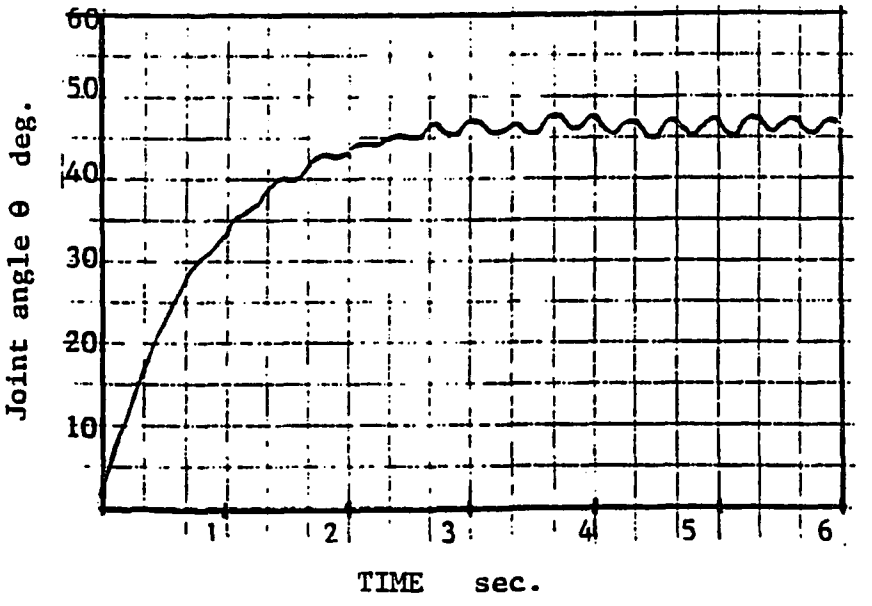

Figure 16